PHYSIOLOGICAL MODELS, DEVELOPMENT

Modeling is an important facet of engineering. Models are simplified representations of real-world systems. For this reason, models are also an important part of everyday life. If you wanted to drive from Tucson, Arizona to Madison, Wisconsin you would use a model of the highway system called a road map. Such a map would allow you to understand the highway system of the United States without driving on every road. If you wanted a model of the life of Southern aristocrats at the time of the Civil War, you could use the book *Gone with the Wind.* Highway engineers create models to see how traffic-light synchronization or lane obstructions would affect traffic flow. Ohm's law may be a good model for a resistor. $F = ma$ is a simple model for the movement of a baseball. Models allow us to apply mathematical tools to real-world systems. We use models to understand things that are big, complicated, expensive, or far away in space or time. Certainly, physiological systems fall into some of these categories and are often modeled in the field of biomedical engineering.

Figure 1 shows the relationships between models and the real world. On the extreme left, people do experiments on real-world systems. Baseball players often fit into this category. Over the years, there has been a lot of experimentation with the baseball bat. Most of this experimentation was illegal, because the rules say that (for professional players) the bat must be made from one solid piece of wood. However, to make the bat heavier, George Sisler, who played first base for St. Louis Browns in the 1920s, pounded Victrola phonograph needles into his bat barrel and in the 1950s Ted Kluszewski of the Cincinnati Reds hammered in big nails. To make the bat lighter, many players have drilled a hole in the end of the bat and filled it with cork. Detroit's Norm Cash admitted to using a corked bat in 1961 when he won the American League batting title by hitting .361. However, the corked bat may have had little to do with his success, because he presumably used a corked bat the next year when he slumped to .243. Some players have been caught publicly using doctored bats. In 1974, the bat of Graig Nettles of the Yankees shattered as it made contact, and out bounced six Super Balls. In 1987 Houston's Billy Hatcher hit the ball and his bat split open, spraying cork all over the infield. These are all examples of experimentation with no concrete models to guide them.

To lessen the waste of time and decrement of performance entailed in such experiments with altered bats, we made mathematical models of individual humans. Then we coupled these models to the equations of physics and predicted the ideal bat weight for each individual (2,3). This modeling process is shown in the center box of Fig. 1. However, there is another box labeled *Computer simulation of model* on the right side of Fig. 1. Our model was composed of mathematical equations that we had to solve on a computer. If everything goes right, the digital computer simulation should produce the same results as the mathematical equations. But care must be taken to ensure that this is true. Things that you must worry about include (a) the accuracy of the computer code; (b) numerical factors, such as the integration step size truncation errors, and the integration technique (e.g., quadrature, Adams-Moulton, Runge–Kutta) [see Yakowitz and Szidarovszky (4) for details]; (c) implementation considerations such as using a commercial simulation package that is much bigger than the model, like using a calculator to add single-digit numbers (the point is that in some situations the unused routines could cause problems, like overwriting areas of memory or forcing pointers out of bounds); and (d) the possibility that the hardware is defective (How often do you run the diagnostics on your personal computer?). In our study, we carefully assessed each of these to see how they would affect our predictions about the real world. In addition, matching the output of the model to the real-world system can be a useful experimental approach to numerical validation in general.

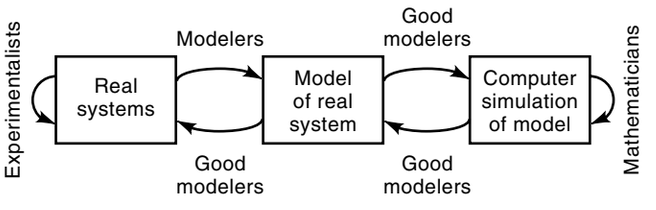

Figure 1. Relationship of systems and models. [Reprinted with permission from W. L. Chapman, A. T. Bahill, and A. W. Wymore, *Engineering Modeling and Design,* Boca Raton, FL: Copyright CRC Press, 1992, p. 45 (Ref. 1).]

Finally, at the extreme right side of Fig. 1 we find pure mathematicians working in the computer world often with no regard to the real world. Early studies of fractals fit into this category. For more on the philosophy and practice of modeling, see Bahill (5).

STEPS IN THE MODELING PROCESS

- Describe the system to be modeled.
- Gather experimental data that describe the behavior of the system to be modeled.
- Investigate alternative models.
- Make the model.
- Validate the model.
  - Show that the model behaves like the physical system.
  - Use the model to simulate something that was not used in its design.
  - Perform a sensitivity analysis.
- Show how the model interacts with models for other systems.
- Analyze the performance of the model.
- Reevaluate and improve the model.
- Suggest new experiments for the physical system.

Modeling is not a serial process; some steps can be done in parallel and it is very iterative. This prescription for describing processes was developed by Bahill and Gissing (6).

DESCRIBE THE SYSTEM TO BE MODELED

The control of movement has long been an enigma for scientists as well as for parents who marvel at the miracle of seeing their children take their first steps. The control of muscles that we often take for granted is so complex that it is difficult to comprehend the intricacies involved. To develop an understanding of such complex movement control systems, we

started with a study of a simple neuromuscular system, developed physiologically realistic models, and then refined these models.

The eye movement system is a good starting point because of its simplicity, relative to other neuromuscular systems. This system has primarily two degrees of freedom, namely, horizontal and vertical; and only two muscles are involved in horizontal eye movements, as compared with six or more degrees of freedom and about 30 major muscles for each leg involved in locomotion. The study of the eye movement system is also aided by the ease with which the movements can be measured. Any knowledge gained in the control of eye movements will contribute not only to the understanding of the oculomotor system but also to the understanding of larger, more complex neuromuscular systems.

The purpose of the eye movement system is to keep the fovea, the region of the retina with the greatest visual acuity in daylight, on the object of interest. To accomplish this task, the following four types of eye movements work in harmony: *saccadic eye movements,* which are used in reading text or scanning a roomful of people; *vestibulo-ocular eye movements,* used to maintain fixation during head movements; *vergence eye movements,* used when looking between near and far objects; and *smooth-pursuit eye movements,* used when tracking a moving object. These four types of eye movements have four independent control systems, involving different areas of the brain. Their dynamic properties, such as latency, speed, and bandwidth, are different, and they are affected differently by fatigue, drugs, and disease.

The specific actions of these four systems can be illustrated by the example of a duck hunter sitting in a rowboat on a lake. He scans the sky using saccadic eye movements, jerking his eyes quickly from one fixation point to the next. When he sees a duck, he tracks it using smooth-pursuit eye movements. If the duck lands in the water right next to his boat, he moves his eyes toward each other with vergence eye movements. Throughout all this, he uses vestibulo-ocular eye movements to compensate for the movement of his head caused by the rocking of the boat. Thus, all four systems are continually used to move the eyes.

This section is primarily about developing and validating a model for the human smooth-pursuit eye movement system. Other systems are only included when they interact with the smooth-pursuit system.

GATHER EXPERIMENTAL DATA THAT DESCRIBE THE BEHAVIOR OF THE SYSTEM TO BE MODELED

Experiments with transient movement target waveforms reveal a 150 millisecond (ms) time delay in the human smooth-pursuit eye movement system (7). The effects of this time delay are apparent during starting and stopping transients, as shown in Fig. 2 (8). However, when a human (or a monkey) tracks a target that is moving sinusoidally, the subject quickly locks onto the target and tracks with neither latency nor phase lag. It is as if the subject creates an internal model of the target movement and uses this model to help track the target. This internal model has been called a predictor (9–11), a long-term learning process (12), a percept tracker (13–16), a neural motor pattern generator (17), and a target-selective adaptive controller (8,18–20).

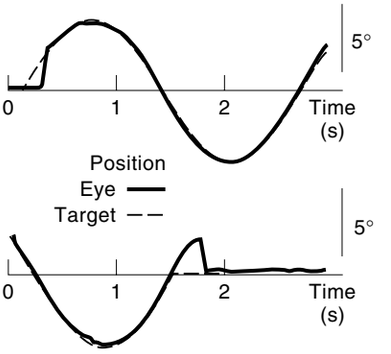

Figure 2. Typical beginning (top) and ending (bottom) of sinusoidal tracking. When the target (dashed line) started there was a 150 ms delay before the eye velocity increased; when the target stopped there was a 120 ms delay before the eye velocity began to decrease. Target movements were ±5° from primary position. The time axis is labeled in seconds, and upward deflections represent rightward movements. [Reprinted from A. T. Bahill and J. D. McDonald, Smooth pursuit eye movements in response to predictable target motions, *Vision Res.,* **23**: 1573–1583, 1983, with permission from Elsevier Science. (Ref. 8).]

The Sinusoidal Target Waveform

The sinusoid is the most common smooth-pursuit target waveform because it is easy to generate and easy to track. Our sinusoidal target waveform is given by $r(t) = A \sin \omega t$. Our normal amplitude, A, was 5° (i.e., ±5° from primary position).

Figure 2 (top) shows tracking of the beginning of sinusoidal movement. Smooth pursuit began 150 ms after the target started to move. It was followed by a corrective saccade at 200 ms and then by zero-latency, unity-gain tracking. Figure 2 also shows a termination of sinusoidal smooth-pursuit tracking. The smooth-pursuit velocity started declining 120 ms after the target velocity dropped. It reached zero velocity at 220 ms, when a corrective saccade occurred to end the subject's tracking. Thus, the beginning and ending transients show the effects of the time delay, whereas steady-state tracking does not.

The Cubic Target Waveform

Humans can overcome a large internal time delay and track sinusoidal target waveforms with unity gain and no time delay. Moreover, they learn to do this very quickly. To help determine if humans can easily track every predictable waveform, we created a cubic waveform. The cubic waveform is simple, but we could not imagine a naturally occurring cubic visual target.

We used the cubical target waveform (shown in Fig. 3) because no naturally occurring visual targets move with a periodic cubical waveform; thus, our results were not influenced by previous learning; yet, the cubical waveform resembles a sinusoid so it should be possible to track. The cubical target waveform was formed with the following third-order polynomial:

$$r(t) = 10.39A\left[2\left(\frac{t^3}{T}\right) - 3\left(\frac{t^2}{T}\right) + \left(\frac{t}{T}\right)\right] \qquad \text{for } 0 < t < T$$

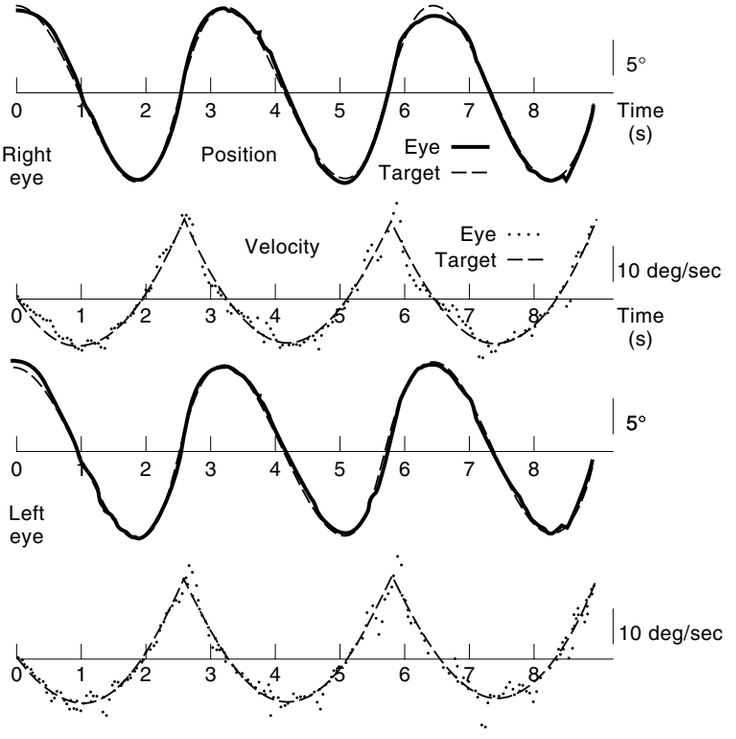

Figure 3. Binocular eye movements for good tracking of the cubical target waveform. [From D. E. McHugh and A. T. Bahill, Learning to track predictable target waveforms without a time delay, *Invest. Ophthalmol. Vis. Sci.,* **26**: 933, 1985. (Ref. 21).]

where T represents target period and A is the amplitude. Previous studies have shown that humans track well when the target has an amplitude of 5° and a frequency of about 0.32 Hz, so these values were used in our experiments. The target always started with zero phase and zero offset. No warning was given before the target started. Another benefit of the cubic waveform is that it looks like a sinusoid but the velocity is strikingly different. Therefore, by analyzing the eye velocity records we could tell if the subject had really learned the cubical waveform or if he had merely approximated it with a sinusoid.

Figure 3 shows excellent tracking of the cubical target waveform. Using only smooth-pursuit eye movements, the subject was able to keep the fovea on the target for over 8 s. Saccades were not removed or filtered out of the eye position traces; indeed small conjugate saccades can be seen at the 8.5 s mark.

Learning to Track the Cubical Waveform

Figure 3 shows that a human can track the cubic target waveform very well. But this capability is not inherent. It must be learned. Our standard learning protocol began with a 6 s square-wave calibration target waveform, followed by 9 s of the cubical target waveform, 3 s of the square-wave target waveform, another 9 s of the cubical waveform, and finally another 6 s of the square-wave calibration target waveform. The subjects were allowed to rest for 5 min and then the sequence was repeated. This process continued for about 2 h.

Because the purpose of the eye movement control system is to keep the fovea on the target, we felt that the error between the eye and the target was the most appropriate measure of the quality of tracking. Our primary metric was the mean-square error (MSE) between eye position and target position. The human fovea (specifically the inner foveal pit) has a radius of 0.5° (17,22). Therefore, a target consistently on the outer edge of the fovea produces an MSE of $0.25^{\circ 2}$.

Single and double exponential curves were fit to the MSE data. The best fit was usually an exponential of the form $\text{MSE} = Ae^{-Bt} + C$. The solid lines of Fig. 4 show the exponential curves fit to the data of our four best-tracking college stu-

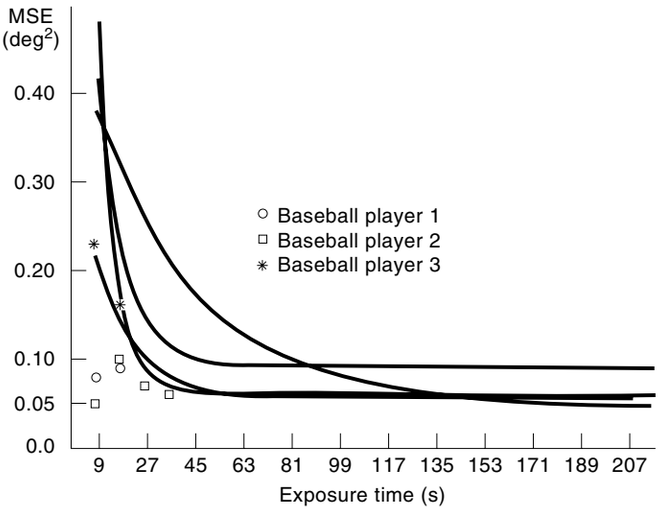

Figure 4. Time course of learning for seven subjects. Solid lines are the exponential curves fit to the data of our four best-tracking college students. Circles, asterisks, and squares are data points for three professional baseball players. [From D. E. McHugh and A. T. Bahill, Learning to track predictable target waveforms without a time delay, *Invest. Ophthalmol. Vis. Sci.,* **26**: 935, 1985. (Ref. 21).]

dents. We were trying to quantify the ultimate capabilities of the human smooth-pursuit system, so we only report the performance of our best subjects. In this figure, we only show data of four of 20 college students. The other students did not demonstrate such low-error tracking.

To narrow in on this exquisite tracking performance we decided to study optimal humans performing optimally. Who is an optimal human? For eye tracking capability, we thought professional athletes would fit the bill. So we invited some professional baseball players to participate in our experiments. The MSEs for three members of the Pittsburgh Pirates Baseball Club are represented by circles, asterisks, and squares in Fig. 4. In viewing the target for the first time, professional baseball players 1 and 2 had much smaller MSEs (0.05 and 0.08) than our other subjects. They had never seen a cubical waveform before, yet they started out with low MSEs. Baseball players 1 and 2 played in the major leagues for over 10 years. Player number 3 never got out of the class A Farm System. These data seem to indicate that the ability to track the cubical waveform is correlated with the ability to hit a baseball.

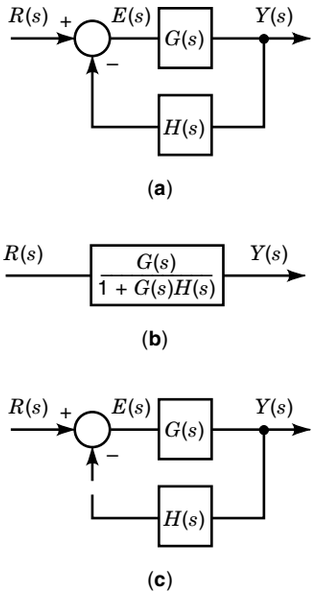

Figure 5. (a) A closed-loop feedback control system, (b) an equivalent representation, and (c) the closed-loop system with its loop opened. Many analysis techniques require the study of the open-looped system of (c). [From A. T. Bahill, *Bioengineering: Biomedical, Medical and Clinical Engineering,* 1981, p. 215. Reprinted with permission of Prentice-Hall, Upper Saddle River, NJ. (Ref. 5).]

DEVELOPING THE MODEL

Most physiological systems are closed-loop negative-feedback control systems. For example, consider someone trying to touch his or her nose with a finger. He or she would command a new reference position and let the arm start to move. But before long, sensory information from the visual and kinesthetic systems would signal the actual finger position. This sensory feedback signal would be compared to the reference or command signal to create the error signal that drives the arm to the commanded output position.

In the analysis of such systems, it is difficult to see which effects in the output are due to elements in the forward path and which are due to sensory feedback. In order to understand the contribution of each element, it is necessary to open the loop on the system—that is, to remove the effects of feedback. For some systems it is easy to open the feedback loop, while for others it is exceedingly difficult since some systems have multiple or even unknown feedback loops. It is easy to open the loop on the human eye movement system.

Many investigators have studied the human smooth-pursuit eye movement system under open-loop conditions; these studies have helped us understand this system. However, some investigators reported varied and inconsistent responses; they found open-loop responses idiosyncratic. It is suggested that the reason for these difficulties is that physiological systems, unlike man-made feedback control systems, are capable of changing their control strategy when the control loop is opened. Several specific changes in eye movement control strategy are shown in this section. Although the specific system studied was the eye movement system, the technique presented should generalize to other physiological systems.

Opening the Loop on a System

A linear system can be schematically represented as a closed-loop system, as shown in Fig. 5(a). In this figure, R represents the reference input, and Y is the output. The output is measured with a transducer, H, and the resulting signal is subtracted from the input to yield the error signal, E. In many systems (such as the oculomotor systems), the element in the feedback loop, H, is unity; therefore the output is compared directly with the input, which explains the reason for calling the resultant the error. This error signal is the input for the main part of the system represented by G. This is called a *closed-loop system* because of the closed loop formed by G, H, and the summer. This system can be redrawn as shown in Fig. 5(b). Although the transfer function of this equivalent system describes the input–output relationship of the system, it is not very useful for modeling physiological systems because it hides specific behavior by lumping everything into one box. On the other hand, important information about the system's performance can be gained by techniques that examine components within the loop. One such technique for studying a system is to "open the loop," as shown in Fig. 5(c), and then study the response of this open-looped system. The open-loop transfer function is defined as the total effect encountered by a signal as it travels once around the loop. That is, the open-loop transfer function is $G_{ol} = GH$.

Note that this is not the input–output transfer function of the system with its loop opened (which would be G), nor is this the transfer function of the equivalent redrawn closed-loop system shown in Fig. 5(b). When we open the loop on a closed-loop system, bizarre behavior often results. In response to a step disturbance, a closed-loop system with its loop opened will usually vary its output until it is driven out of its normal operating range. For instance, if R in Fig. 5(c) is a step and G is a pure integrator, the error will be constant and the output will increase until the system reaches its limit of linearity.

Often the success of a systems analysis depends on being able to open the loop on a system. If it is an electrical circuit,

one might merely cut a wire. However, if it is a human physiological system, such an approach is not feasible, and other techniques must be developed. Such techniques usually involve manipulating the variable normally controlled by the system, so that the feedback is ineffective in changing the error signal. For example, in the physiological sciences, some of the earliest examples of opening the loop are the voltage clamp technique developed by Marmount (23) and Cole (24), wherein they measured the voltage and injected current to keep the voltage constant, and the light modulation technique used by Stark to study the human pupil (25). In the voltage clamp technique the experimenters fixed the voltage across a neuronal membrane, the parameter that is normally controlled by the neuron: Although it struggled to open and close the ionic channels, the neuron could not regulate the membrane voltage, and therefore the loop was opened. In the case of the pupil of the eye, the experimenters controlled the amount of light falling on the retina: Although it struggled to open and close the pupil, the pupillary system could not control the amount of light falling on the retina, and thus the loop was opened. Similarly, the use of force and length servos in research on motor systems provides a means of examining components within feedback loops, although setting up these studies is complicated by the multiplicity of feedback loops in these systems (see, for example, Ref. 26).

We think these open-loop techniques can be used in a broad range of physiological systems. Of course, nothing is easy and some problems must be overcome. In many systems, the difficulties lie in trying to isolate one system so that others do not interfere, as in the previously mentioned pupillary and motor control systems. In other cases, the difficulty lies in opening the loop on the system. For example, if the output of the respiratory system is defined to be the ventilation rate, then one could study the open-loop behavior of the system by controlling the concentration of the gases being breathed while monitoring the ventilation rate. However, when modeling a different aspect of this system, such that a different quantity is defined as the output, opening the loop would become difficult: For example, controlling the venous concentration of CO_2 would be difficult.

Physiological systems often have several parallel feedback loops (e.g., hormonal and neural) acting simultaneously. One of the greatest challenges in studying a physiological control system is that one may not even be aware of all the feedback pathways.

Opening the Loop on the Eye Movement Control System

An easy way to open the loop on the eye movement system is to stabilize an object on the retina. This can be done, for example, by looking a few degrees to the side of a camera when someone triggers a flash. There will be an afterimage a few degrees off your fovea. Try to look at the afterimage: You will make a saccade of a few degrees, but the image (being fixed on the retina) will also move a few degrees. You will then make another saccade, and the image will move again. Thus, no matter how you move your eye, you cannot eliminate the error and put the image on your fovea. This is the same effect as if someone opened the loop on an electronic system by cutting a wire [as in Fig. 5(c)]. Therefore, this is a way of opening the loop on the eye movement system. There is also another simple way to study open-loop saccadic behavior. Gaze at the blue sky on a sunny day and try to track your floaters (sloughed collagen fibers in the vitreous humor). These hairlike images move when the eye moves; therefore your initial saccades will not succeed in getting them on the fovea. However, with a little practice, one can learn to manipulate these images, because they are not fixed on the retina and a human can rapidly learn to manipulate the system. This latter point often confounds attempts to open the loop on a physiological system. When the experimenter attempts to open the loop, the human quickly changes control strategy, thereby altering the system under study.

The most common experimental technique for opening the loop on the eye movement system, pioneered by Young and Stark (27), employs electronic feedback as shown in Fig. 6. In operation, the target is given a small step displacement, say 2 degrees to the right. After about 200 ms, the eyes saccade 2° to the right. During this movement, the target is moved 2° farther to the right, so that at the end of the saccade the target is still 2° to the right. After another 200 ms delay, the eyes saccade another 2° to the right, and the target is moved another 2°, thereby maintaining the 2° retinal error. The saccadic eye movements are not effective in changing the retinal error; therefore, the loop has been opened. In this open-loop experiment, the subject produces a staircase of 2° saccades about 200 ms apart, until the measuring system becomes nonlinear. Such a staircase of saccades is shown in the beginning of Fig. 7.

Electronic feedback has also been used to open the loop on the smooth-pursuit system. In these experiments, the target was moved sinusoidally. When the eye moved attempting to track the target, the measured eye position signal was added to the sinusoidally moved target position (as shown in Fig. 6). Thus the eye movements became ineffective in correcting the retinal error and the feedback loop was, in essence, opened. In contrast to open-loop saccadic experiments, open-loop smooth-pursuit experiments do not stabilize the image on the retina, but rather the target is moved across the retina in a controlled manner by the experimenter. This is done because the

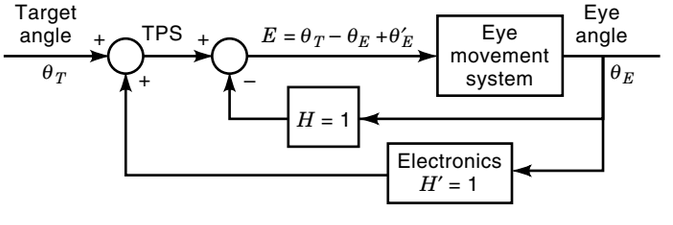

Figure 6. Electronic technique for opening the loop on the human eye movement system. The position of the eye, θ_E, is continuously measured and is summated with the input target signal, θ_T. For the eye movement system $H = 1$, because if the eye moves 10°, the image on the retina also moves 10°. If the eye movement monitor and associated electronics are carefully designed so that $H' = 1$, then any change in actual eye position, θ_E, is exactly canceled by the change in measured eye position, θ'_E. Thus the error signal, E, is equal to the target signal. This is the same effect as if the feedback loop had been cut, as in Fig. 5(c). The target position in space (TPS) is the sum of the input signal and the measured eye position; care must be taken to keep this position within the linear range of the eye movement monitor. [From A. T. Bahill and D. R. Harvey, Open-loop experiments for modeling the human eye movement system, *IEEE Trans. Syst. Man Cybern.,* **SMC-15**: 241, © 1986 IEEE (Ref. 30).]

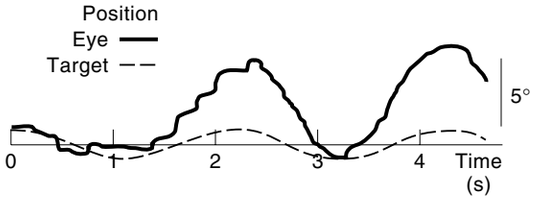

Figure 7. Position of the target and eye as functions of time for typical human open-loop tracking. After the feedback loop was opened, and the 1-sec mark, the subject made a series of saccades trying to catch the target. When this strategy did not work, he seemed to turn off the saccadic system and produce only smooth-pursuit eye movements. This subject was experienced in oculomotor experiments. The large open-loop gain appears to be a characteristic of such experienced subjects. [From A. T. Bahill and D. R. Harvey, Open-loop experiments for modeling the human eye movement system, *IEEE Trans. Syst. Man Cybern.,* **SMC-15**: 248, © 1986 IEEE (Ref. 30).]

saccadic system is a position tracking system and retinal position must be controlled, whereas the smooth-pursuit system is a velocity tracking system and retinal velocity must be controlled.

Results of Open-Loop Experiments on the Smooth-Pursuit System

Open-loop experiments should provide results that not only describe the characteristics of elements within the feedback loop, but also provide a description of the system's performance under closed-loop conditions. Consequently, similarity of actual closed-loop behavior with that predicted from open-loop data is indication of the success of the investigation. Such agreement has been found by Wyatt and Pola (28,29) in experiments in which subjects tracked sinusoidal waveforms. Although idiosyncratic differences were found between their subjects, agreement was found between actual and predicted closed-loop behavior for individual subjects. However, subsequent investigators were not able to replicate their results (16). And in other studies (30,31), individualistic behavior was varied enough to obviate any meaningful description of the system using such data.

Several factors can be indentified that possibly contribute to the differences between individual subjects and between different experiments. One such factor is the predictability of the target waveform used in testing. While Wyatt and Pola (28) used predictable sinusoidal waveforms and obtained consistent results, Collewijn and Tamminga (31) used a pseudorandom mixture of sinusoids and found great variability between subjects. However, sinusoids were also used by Harvey (30) with inconsistent results between subjects. Another factor may be the influence of prior experience on subject performance. Examining the results from several studies (28,30,31) reveals that open-loop gains are larger in subjects with more experience in laboratory tracking tasks.

The one common element shared by these studies is intersubject variability, although the magnitude of this variability differed considerably. It is noteworthy that such variability is found not only between subjects, but also in the performance of individual subjects in single trials. Such variation has been observed by Harvey (30) and also by Leigh et al. (32), in a subject in which open-loop behavior was observed by presenting a visual target to a patient's paralyzed eye while monitoring the motion of the normal, but covered, eye. Each subject's performance also depends on the instructions given to the subject (33). These findings show that the variability inherent in open-loop studies is attributable not only to differences between subjects but also to time-varying performance of individual subjects.

Comparing Open-Loop Experiments with Simulations

Insight into the behavior of the smooth-pursuit system under open-loop conditions was sought by Harvey (30) through a comparison of experimental results with those from simulations. The simulations were performed using the target-selective adaptive control (TSAC) model (19) shown in Fig. 8. This model has three branches. The top branch, the saccadic branch, generates a saccade after a short delay whenever the disparity between target and eye position is too great. The middle branch, the smooth-pursuit branch, produces smooth tracking of moving targets. The input to the smooth-pursuit branch is velocity, so the first box (labeled smooth-pursuit processing) contains a differentiator and a limiter. The box

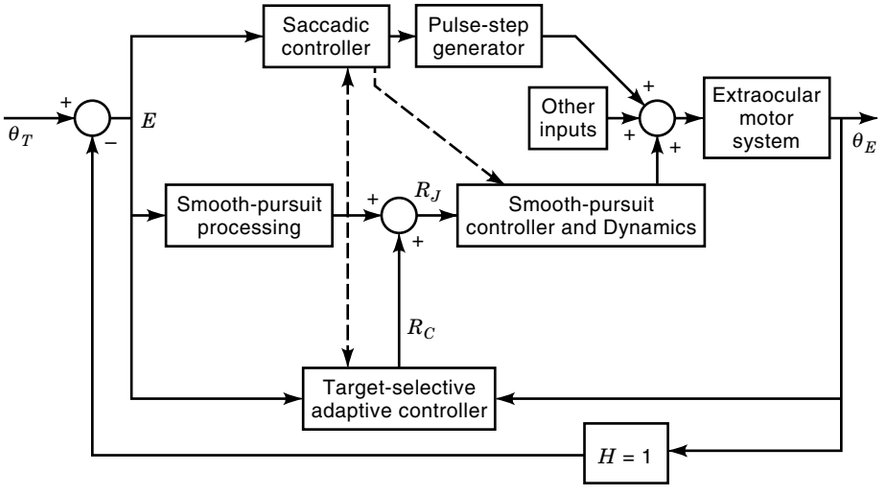

Figure 8. The general form of the TSAC model. [From A. T. Bahill and T. M. Hamm, Using open-loop experiments to study physiological systems with examples from the human eye movement systems, *News Physiol. Sci.,* **4**: 107, 1989 (Ref. 56).]

labeled smooth-pursuit controller and dynamics contains a first-order lag (called a leaky integrator), a gain element, a time delay, a saturation element, and an integrator to change the velocity signals into the position signals used by the extraocular motor system. The bottom branch contains the target-selective adaptive controller that identifies and evaluates target motion and synthesizes an adaptive signal, R_c, that is fed to the smooth-pursuit branch. This signal permits zero-latency tracking of predictable visual targets, which the human subject can do, despite the time delays present in the oculomotor system. The adaptive controller must be able to predict future target velocity, and it must know and compensate for the dynamics of the rest of the system. The adaptive controller is separate from the smooth-pursuit system in the model and also in the brain (11). The adaptive controller sends signals to the smooth-pursuit system and also other movement systems (34). All of these branches send their signals to the extraocular motor system, consisting of motoneurons, muscles, the globe, ligaments, and orbital tissues. And of course, the final component of the model is a unity gain feedback loop that subtracts eye position from target position to provide the error signals that drive the system. The solid lines in this figure are signal pathways, while the dashed lines are control pathways. For instance, the dashed line between the saccadic controller and the smooth-pursuit controller carries the command to turn off integration of retinal error velocity during a saccade.

In the experiments, many different target waveforms are used. The step target was presented to the subject to verify that the technique of opening the loop using electronic feedback was working. Because the step target introduced a position error rather than a velocity error, this experiment opened the loop on the saccadic system rather than the pursuit system. A position error with the feedback loop opened should have elicited a staircase of saccades. If this expected open-loop response to the step target was seen, then the electronic feedback was opening the loop correctly, as between 1.5 s and 2.5 s of Fig. 7.

There was difficulty in getting consistent results for sinusoids with the loop opened. The most consistent results obtained for such presentations came from the first few seconds after the loop has been opened. This finding suggests that the difficulties with open-loop sinusoids were probably due to the involvement of high-level processes such as adaptation. Once the loop was opened, the behavior of the target changed. Often the subjects would appear to respond to this change in target behavior by changing their tracking strategies. Figure 7 shows a presumed example of such a change in human tracking strategy. Between 1.5 s and 2.5 s of this record the subject behaved as one would expect for a subject tracking an open-loop target; there is a saccade every 200 ms (approximately the time delay before the saccadic system responds to a position error). However, in the middle of the record, the saccades cease; it seems that the subject turned off the saccadic system. Such saccade free tracking was common in these experiments and in other open-loop experiments (16,28,29,32,33,35). The records are strikingly devoid of saccades in spite of the large position errors, a finding that, oddly, received little comment by previous investigators (except for Ref. 33), although it is often seen in the data.

By way of comparison, the model is shown tracking a sinusoid under open-loop conditions in Fig. 9. To simulate the

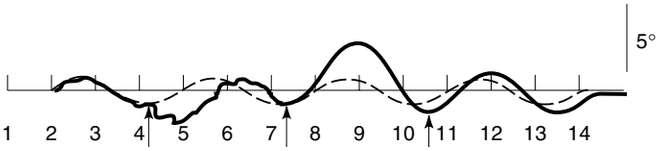

Figure 9. Position of the target (dashed) and model (solid) as functions of time under a variety of conditions. At the first arrow, the loop was opened, at the second arrow the saccadic system was turned off, and at the third arrow the adaptive controller was turned off. Tracking patterns similar to each of these are common in human records. [From A. T. Bahill and D. R. Harvey, Open-loop experiments for modeling the human eye movement system, *IEEE Trans. Syst. Man Cybern.,* **SMC-15**: 249, © 1986 IEEE (Ref. 30).]

changes in strategy that are apparent in the human data of Fig. 7, the model characteristics were changed at intervals. From 2 to 4.25 s there is normal closed-loop tracking. At 4.25 s the loop was opened, the adaptive controller was turned off, and the smooth-pursuit gain was reduced to 0.7, thus producing a staircase of saccades similar to those shown in Fig. 7. At 7.25 s the saccadic system was turned off, the adaptive controller was turned back on, and the gain of the smooth-pursuit system was returned to its normal value; the model tracked with an offset similar to that of Fig. 7. This type of position offset was often noticed in human subjects during open-loop tracking. Finally, at 10.5 s the adaptive controller was turned off and the model tracked without an offset but with a time delay as was seen in some subjects.

These simulations help explain some confusing data in the literature by allowing us to suggest that when the loop on the human smooth-pursuit system is opened, subjects alter their tracking strategy to cope with altered target behavior. Some subjects continue to track with all systems (producing a staircase of saccades), some turn off the saccadic system (producing smooth tracking with an offset), some also turn off the adaptive controller (producing smooth tracking without an offset), and some change the gain on the smooth-pursuit system. Thus, each subject appears to adapt to the novel tracking task created by opening the loop by selecting subcomponents of the smooth-pursuit system and/or changing parameters within those subsystems. All these strategy changes are within the possibilities provided by the model.

Multifaceted control is also common in other physiological systems (see, for example, Refs. 36 and 37). Thus, the potential exists in other physiological control systems for changes in strategy—that is, a change in the balance of control subsystems in different physiological states whether these states occur "naturally" or are imposed by an investigator. Such changes may occur in different behavioral states as observed, for example, for respiratory control in the newborn (38). Consequently, it should not be surprising that when an investigator attempts to open the loop on a control system the control strategy changes. This section demonstrates this principle for the eye movement system.

The technique of opening the loop on a physiological system in order to better understand its behavior is very powerful as long as care is taken to acknowledge that the human is a complex organism and is likely to change its behavior when the input changes its behavior.

MAKE THE MODEL

The human can overcome a time delay and track visual targets with zero latency. This is nicely demonstrated by the smooth-pursuit eye movement system. We found that if our model was to emulate the human, it had to predict target velocity and compensate for system dynamics. The model accomplished this using a prediction algorithm. To help validate the model, a sensitivity analysis and a parameter estimation study were performed.

Figure 10 shows our model for the human eye movement systems. Like the human, this model can overcome the time delay and track a target without latency. To do this, the model must be able to predict future target velocity and compensate for system dynamics. In this section, a least-mean-square technique for predicting target velocity is described. After incorporating this prediction algorithm into the model, the model was studied to learn more about the model, and hopefully about the human. In particular, we performed a sensitivity and analysis of the predictor and then investigated how parameter variations affected the MSE between the predicted output and the actual target waveform.

The TSAC Model

This section primarily examines the smooth-pursuit eye movement system. The earliest model for the smooth-pursuit system is the sampled data model developed by Young and Stark (27). Because of later evidence presented by Robinson (39) and Brodkey and Stark (40), the pursuit branch is no longer viewed as a sampled data system, but rather as a continuous one.

There is one physically realizable model capable of overcoming the time delay in the smooth-pursuit branch, the TSAC model developed by McDonald (18,19). This model with the saccadic and smooth-pursuit branches and their interactions is shown in Fig. 10.

Referring to Fig. 10, the input to the smooth-pursuit branch is retinal error, which is converted to velocity by the differentiator. The limiter prevents any velocities greater than 70°/s from going through this branch. [The numbers given in this section are only typical values, and the standard deviations are large—for example, and LaRitz (41) showed smooth-pursuit velocities of 130°/s for a baseball player.] The leaky integrator $K/(\tau s + 1)$ is suggested from (a) experimental results showing that humans can track ramps with zero steady-state error (7) and (b) open-loop experiments that showed a slope of −20 dB per decade for the pursuit branch's frequency response (30). The gain, K, for the pursuit branch must be greater than unity, since the closed-loop gain is almost unity. Currently used values for the gain are between 2 and 4 (30,42). The e^{-sT} term represents the time delay, or latency, between the start of the target movement and the beginning of pursuit movement by the subject. A time delay of 150 ms is currently accepted (30,33). The saturation element prevents the output of any velocities greater than 60°/s, the maximum velocity produced by most human smooth-pursuit systems.

The model must be able to overcome the 150 ms time delay and track with zero latency. Because the smooth-pursuit system is a closed-loop system, the model's time delay appears in the numerator and the denominator of the closed-loop transfer function,

$$\frac{\dot{\theta}_E}{\dot{\theta}_T} = \frac{Ke^{-sT}}{\tau s + 1 + Ke^{-sT}}$$

An adaptive predictor using adaptive filters was designed to overcome the time delay in the numerator. Compensation for the model's dynamics overcomes the time delay in the denominator.

We used several different techniques for predicting target velocity. There are many more to choose from (see the "ADAPTIVE FILTERS" and "FILTERING THEORY" sections of this encyclopedia). Now we will make a detailed presentation of one of these prediction techniques. The nonmathematical reader may skip this section (all the way to "VALIDATE THE MODEL") without loss of continuity.

The Least-Mean-Square Adaptive Filter

The least-mean-square (LMS) adaptive filter, popularized by Widrow (43–45), is a self-designing filter composed of a

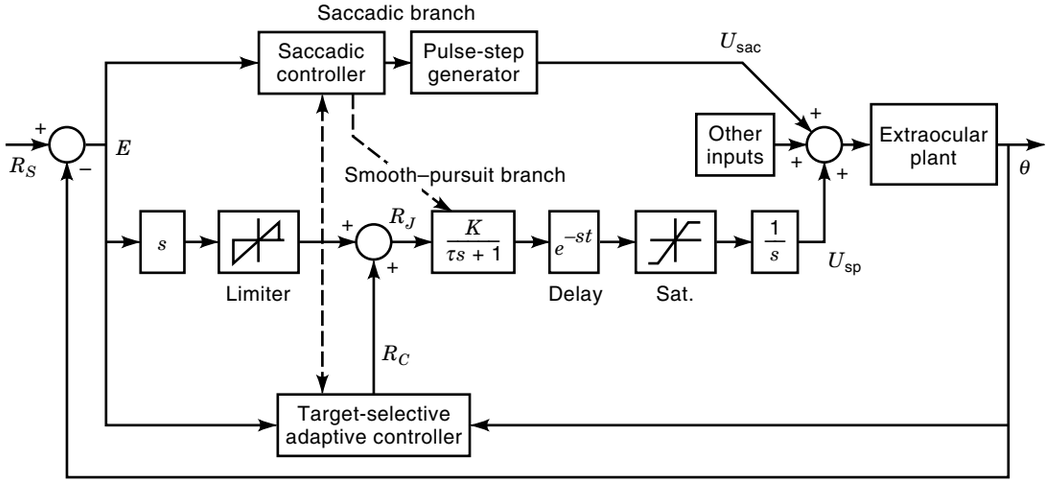

Figure 10. McDonald's TSAC model has three branches: smooth pursuit, saccadic, and the adaptive predictor.

tapped delay line, variable weights, a summing junction to add the weighted signals, and machinery to adjust the weights. Two processes occur in the adaptive filter: the adaptation process and the operation process.

The *adaptation process* handles weight adjustment. The values of the weights are determined by estimating the statistical characteristics of the input and output signals. The heart of the adaptation process is the weight adjustment algorithm. As each new input sample is received, the weights are updated by the algorithm,

$$\boldsymbol{W}(j+1) = \boldsymbol{W}(j) - k_x \nabla[E^2(j)]$$

where

$\boldsymbol{W}(j+1)$ = the weight vector after adaptation
$\boldsymbol{W}(j)$ = the weight vector before adaptation
k_s = the proportionality constant controlling stability and the rate of convergence
$E(j)$ = the difference between the desired response and the filter's output, the error
$\boldsymbol{X}(j)$ = the vector of input signals
$\nabla[E^2(j)]$ = the gradient of the error squared with respect to $\boldsymbol{W}(j)$

In order to find the best possible weights, we computed the gradient (with respect to $\boldsymbol{W}$) of the squared error, set this equal to zero, and solved for the optimum weights. The result is the Weiner–Hopf equation:

$$\boldsymbol{W}_{\text{LMS}} = \phi^{-1}(x,x)\phi(x,d)$$

where

$\boldsymbol{W}_{\text{LMS}}$ = the vector of weights that would give the LMS error
$\phi(x, x)$ = autocorrelation matrix of the input signals
$\phi(x, d)$ = covariance matrix between the input signal and the desired output signal

To solve the Wiener–Hopf equation it is necessary to compute the correlation matrices. However, this would require a lot of computer time; furthermore, these matrices cannot be computed in advance, because this would require *a priori* knowledge of the statistics of the input signal.

Because it is difficult to compute the true gradient, we use an estimate of the gradient, which is equal to $-2E(j)X(j)$. Our algorithm is a form of the method of steepest descent using estimated gradients instead of measured gradients. Using this estimated gradient, the adjustment algorithm can be written as

$$\boldsymbol{W}(j+1) = \boldsymbol{W}(j) + 2k_s E(j)\boldsymbol{X}(j)$$

Figure 11 illustrates the implementation of this weight adjustment algorithm. If the input signals are uncorrelated, then the expected value of the estimated gradient converges to the true gradient without any knowledge of the input signal's statistics.

During the *operation process* of the LMS filter, illustrated in Fig. 12, the tapped delay-line input signals are weighted, using the gains from the adaptation process and summed to form the output signal. The difference between the desired output signal and the actual output of the filter is the error that is fed back to the weight adjustment algorithm.

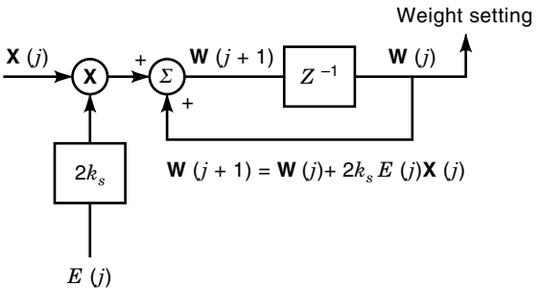

Figure 11. Implementation of the weight adjustment algorithm. [From D. R. Harvey and A. T. Bahill, Development and sensitivity analysis of adaptive predictor for human eye movement model, *Transaction of the Society for Computer Simulation,* December 1985. © 1985 by Simulation Councils, Inc., San Diego, CA. Reprinted by permission. (Ref. 20).]

The speed and accuracy of the filter while converging to the optimal solution depends on several factors. Because noise is introduced into the weight vector from the gradient estimates, it follows that if the filter is allowed to converge slowly, less noise will be introduced during each adaptation cycle and the convergence will be smoother. Regardless of the speed with which the filter converges, some noise will be introduced. This noise prevents the filter from converging to the minimum MSE. The ratio of the excess MSE to the minimum MSE gives a measure of the misadjustment of the filter compared to the optimum system. The misadjustment depends on the time constant of the filter's weights, where the time constant is defined as the time it takes for the weights to fall within 2% of their converged value. A good approximate formula for the misadjustment, M, is

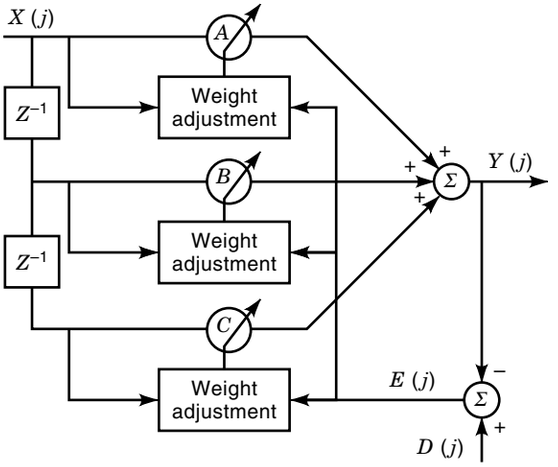

Figure 12. The LMS adaptive filter. The boxes labeled "Weight adjustment" contain systems like Fig. 11. [From D. R. Harvey and A. T. Bahill, Development and sensitivity analysis of adaptive predictor for human eye movement model, *Transaction of the Society for Computer Simulation,* December 1985. © 1985 by Simulation Councils, Inc., San Diego, CA. Reprinted by permission. (Ref. 20).]

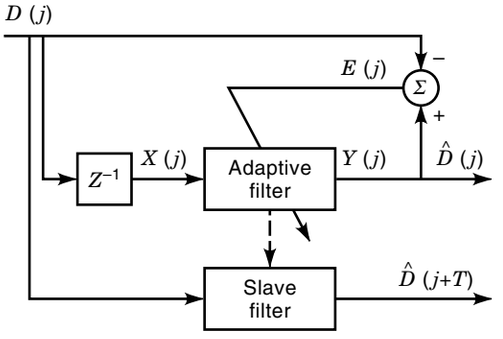

Figure 13. The adaptive predictor. The boxes labeled "Adaptive filter" and "Slave filter" contain systems similar to those in Fig. 12. [From D. R. Harvey and A. T. Bahill, Development and sensitivity analysis of adaptive predictor for human eye movement model, *Transaction of the Society for Computer Simulation,* December 1985. © 1985 by Simulation Councils, Inc., San Diego, CA. Reprinted by permission. (Ref. 20).]

$$M = \frac{n}{4\tau_{\text{MSE}}} \tag{1}$$

This algorithm shows that M is proportional to the number of weights, n, and inversely proportional to the time constant, τ_{MSE}. The time constant τ_{MSE} can be measured experimentally for each simulation. However, we would prefer to find an analytical way to estimate it. We can do that as follows.

To ensure convergence the proportionality constant, k_s, in the weight adjustment algorithm must be within the following bounds:

$$0 < k_s < \frac{1}{\sum_{j=1}^{n} E[X_j^2]}$$

where $E[X_j^2]$ is the expected value of the square of the jth input. For slow and precise convergence, k_s should be within the following more restrictive bounds:

$$0 < k_s \ll \frac{1}{\sum_{j=1}^{n} E[X_n^2]}$$

According to Widrow (43,44), for a filter using tapped delay-line input signals, the time constant is related to the proportionality constant by

$$\tau_{\text{MSE}} = \frac{1}{4k_s E[x^2]} \tag{2}$$

In summary, an adaptive filter is made up of a tapped delay line, variable weights, a summing junction, and the weight adjustment algorithm. The filter adjusts its own internal settings to converge to the optimal solution. Due to noise from the gradient estimate, the accuracy and speed of convergence depends on the number of weights and the proportionality constant, k_s.

The Adaptive Predictor

The adaptive predictor is an application of the LMS adaptive filter. We used this predictor to overcome the 150 msec time delay in the smooth-pursuit model.

Figure 13 shows the design of the adaptive predictor. Two filters are used: an adaptive filter and a slave filter. The adaptive filter determines the appropriate weights. It does this by predicting the value of the input signal 150 ms into the future, $\hat{D}(j + T)$. To accomplish this, the input signal, $D(j)$, is delayed by an amount of time equal to the time to be predicted, in this case 150 ms. This delayed signal, $X(j)$, then serves as the input to the adaptive filter. The filter's weights converge to values that give an output signal, $Y(j)$ or $\hat{D}(j)$, which ideally matches the undelayed input signal.

The slave filter is responsible for predicting. The input to the slave filter is the undelayed signal, $D(j)$. The slave filter is organized like the adaptive filter except there is no automatic adaptation process—that is, no weight adjustment. The weights from the adaptive filter are copied into the slave filter after each adaptation cycle. The output of the slave filter, $\hat{D}(j + T)$, is the predicted value of the input signal at the desired future time.

For the TSAC model, the velocity of the target must be predicted 150 ms into the future to overcome the smooth pursuit system's time delay. Therefore, the target's velocity, the input signal to the predictor, was delayed by 150 ms and used as the adaptive filter's input. Our adaptive filter used between 15 and 150 weights and a proportionality constant of 0.00001. Figures 14 and 15 show the behavior of the predictor with 150 weights. Figure 14 shows the output of the predictor, $\hat{D}(j + T)$, for various target waveforms superimposed on the signal to be predicted. The filter's transients die out within 2.5 s of each abrupt change in velocity.

Figure 15 shows the predictor's MSE, $\|\boldsymbol{E}(j)\|^2$, plotted against the number of iterations of the filter; an iteration was

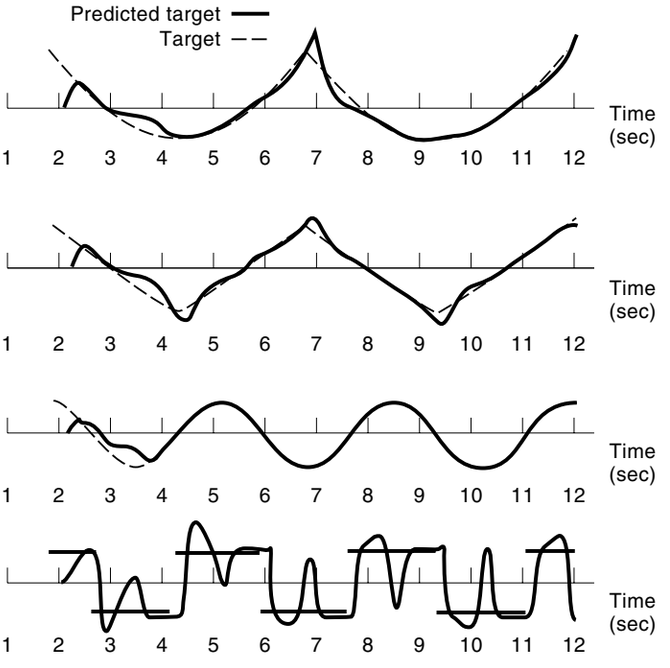

Figure 14. The predictor's output superimposed on the signal it is predicting for four different target velocity waveforms, which are, from top to bottom: parabolic, triangular, sinusoidal, and square. [From D. R. Harvey and A. T. Bahill, Development and sensitivity analysis of adaptive predictor for human eye movement model, *Transaction of the Society for Computer Simulation,* December 1985. © 1985 by Simulation Councils, Inc., San Diego, CA. Reprinted by permission. (Ref. 20).]

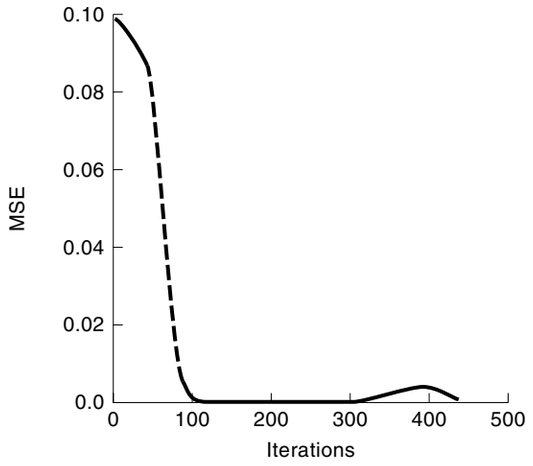

Figure 15. The learning curve for the adaptive predictor. [From D. R. Harvey and A. T. Bahill, Development and sensitivity analysis of adaptive predictor for human eye movement model, *Transaction of the Society for Computer Simulation,* December 1985. © 1985 by Simulation Councils, Inc., San Diego, CA. Reprinted by permission. (Ref. 20).]

completed every 5 ms. After 450 iterations the MSE was effectively zero, which corresponds to 2.25 s. This agrees with the predictor's output in Fig. 14. The settling time of the filter, 450 iterations, is approximately $4\tau_{\text{MSE}}$, where τ_{MSE} is the average time constant for the weights. This gives a τ_{MSE} of 112.5 iterations. Using Eq. (5), $M = n/4\tau_{\text{MSE}}$, the predictor has a misadjustment of approximately 33.3%.

The predicted target velocity from the adaptive predictor compensates for the effects of the time delay in the numerator of the transfer function of Eq. (1). To overcome the effects of the time delay in the denominator, compensation for the model's dynamics must be done. This means that the brain must have a model for itself and the rest of the physiological system, and that it uses this model to generate the required compensation signal.

Compensating for Plant Dynamics

When linear state-variable feedback notation is used for a system, its closed-loop transfer function is

$$\frac{Y(s)}{R_i(s)} = \frac{\boldsymbol{h}'(s\boldsymbol{I} - \boldsymbol{A})^{-1}\boldsymbol{b}Ke^{-sT}}{1 + \boldsymbol{k}'(s\boldsymbol{I} - \boldsymbol{A})^{-1}\boldsymbol{b}Ke^{-sT}} \tag{3}$$

where

Y = system output, θ in Fig. 10
R_i = system input
T = time delay
$\boldsymbol{A}$ = system matrix
$\boldsymbol{b}$ = input coefficient vector
$'$ = vector transpose operation
$\boldsymbol{k}'$ = transposed control vector
$\boldsymbol{h}'$ = transposed output coefficient vector
K = the gain

The general method of compensating for model dynamics is complex. It involves computing an adaptive signal R_a, which, when added to the target position R_s, produces a system input R_i that will produce zero-latency tracking. This method is discussed in detail by McDonald (18,19). We will now briefly show how we used it.

For the human eye movement system the order of the system, the control vector and the output vector are one, so that the following values are appropriate:

$$A = -\frac{1}{\tau}$$
$$b = \frac{1}{\tau}$$
$$h = 1$$
$$k = 1$$

The system's input, $r_i(t)$, is the sum of the target reference signal, $r_s(t)$, and the adaptive signal, $r_a(t)$, that must be computed. To obtain zero-latency tracking, $y(t)$ must equal $r_s(t)$. Putting all of this information into Eq. (3) gives

$$r_s = \frac{(s + 1/\tau)^{-1}(1/\tau)Ke^{-sT}}{1 + (s + 1/\tau)^{-1}(1/\tau)Ke^{-sT}}(r_s + r_a)$$

Solving for r_a gives

$$r_a = \frac{e^{+sT}}{K}(\tau s + 1)r_s \tag{4}$$

The e^{+sT} term shows that predictions must be made. However, the smooth-pursuit system is a velocity tracking system, not a position tracking system, so the controller must be able to predict future values of target velocity. For example, if $\dot{r}_s Y(t)$ is the present target velocity, it must be able to produce $\dot{r}_s Y(t + T)$, where T is the time delay of the smooth-pursuit system. And the controller must modify this prediction to compensate for the dynamics of the system in accordance with Eq. (4). Therefore the compensation signal, R_c, of Fig. 10 becomes

$$r_c(t) = \frac{1}{K}\left[\frac{d}{dt}\tau\dot{r}_s Y(t + T) + \dot{r}_s Y(t + T)\right] \tag{5}$$

This compensation signal allows the smooth-pursuit system to overcome the time delay. To synthesize this signal the adaptive controller must be able to both predict future values of the target velocity and compute first derivatives. These are reasonable computations for the neurons of the human brain. Therefore, Eq. (5) is the algorithm that is in the box of Fig. 10 labeled "Target-selective adaptive controller."

The Sensitivity of the Predictor to Parameter Changes

To determine which parameters have the greatest effect on the model and when they exert their influence, we computed the semirelative sensitivity function, $\tilde{S}^y_\beta$, for each parameter (5,46,47):

$$\tilde{S}^y_\beta = \beta_0 \frac{\partial y}{\partial \beta}$$

where y is the output of the system and β is the parameter that is varied. For this study, we used a fixed perturbation size of +5%. While tracking slowly moving targets the model

is linear and therefore only one perturbation step size was needed (5).

The smooth-pursuit model developed in this study is not independent of other systems. The saccadic system and the adaptive predictor interact with the smooth-pursuit branch. Therefore, we performed the sensitivity analysis twice: once with the saccadic system and the predictor turned on, and again with the saccadic system and the predictor turned off. Eliminating the saccadic system and predictor allowed us to isolate the pursuit branch and study it independently.

The sensitivity of the predictor was studied for three parameters: k_s, the proportionality constant; the number of weights; and the time to be predicted. For k_s and the number of weights, the target waveforms were also changed to determine if the predictor was sensitive to different input signals.

The effect of k_s was found to be the greatest after points of acceleration discontinuities. We performed a sensitivity analysis for many target waveforms, including the four shown in Fig. 14. The influence of k_s is most apparent for the analyses done with the cubic position waveforms. In Fig. 16, we show the results for the cubical target position waveform, which has the parabolic velocity waveform shown in this figure. $\tilde{S}_{k_s}$ peaks at the turnaround points and then begins to taper off to a steady-state value.

Similar results were found for the sensitivity analyses when the number of weights was changed for each target waveform. Figure 17 shows the results of the sensitivity occurs a little later for the weights. $\tilde{S}_n$ is similar for the two parameters, but the time of greatest sensitivity occurs a little later for the weights. This similarity of the two sensitivity functions is reasonable if the misadjustment algorithm of the adaptive filter from Eqs. (1) and (2) is recalled:

$$M = \frac{n}{4\tau_{\text{mse}}} = nk_sE[x^2]$$

This equation shows that a 5% change in either the proportionality constant, k_s, or the number of weights, n, will change the misadjustment of the predictor in a similar manner.

The other parameter changed for the predictor was the prediction time, the desired time to be estimated. The $\tilde{S}$ curve for this case also had the same shape as the curve for the number of weights and the proportionality constant, but its magnitude was smaller.

From these curves, the effect of the predictor can be determined. Changing each parameter by 5% showed that all of them exert their greatest influence right after acceleration discontinuities. Therefore, the predictor's influence will be the greatest at those points.

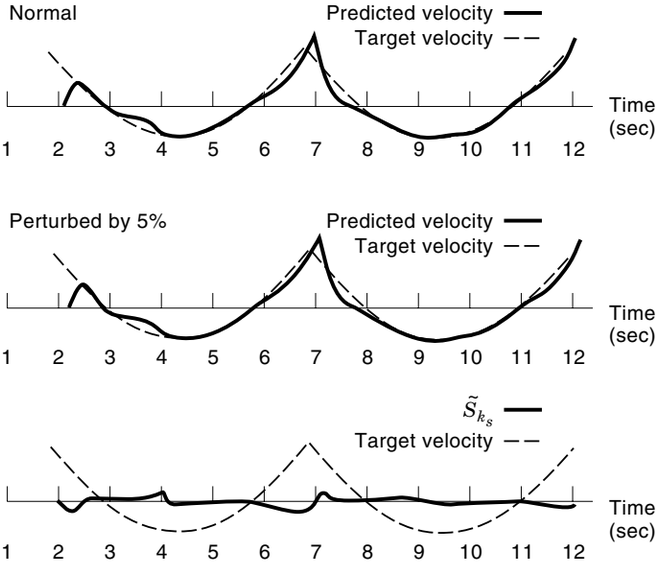

Figure 16. Semirelative sensitivity function of the predictor for changes in the proportionality constant, k_s, for a cubic waveform. [From D. R. Harvey and A. T. Bahill, Development and sensitivity analysis of adaptive predictor for human eye movement model, *Transaction of the Society for Computer Simulation,* December 1985. © 1985 by Simulation Councils, Inc., San Diego, CA. Reprinted by permission. (Ref. 20).]

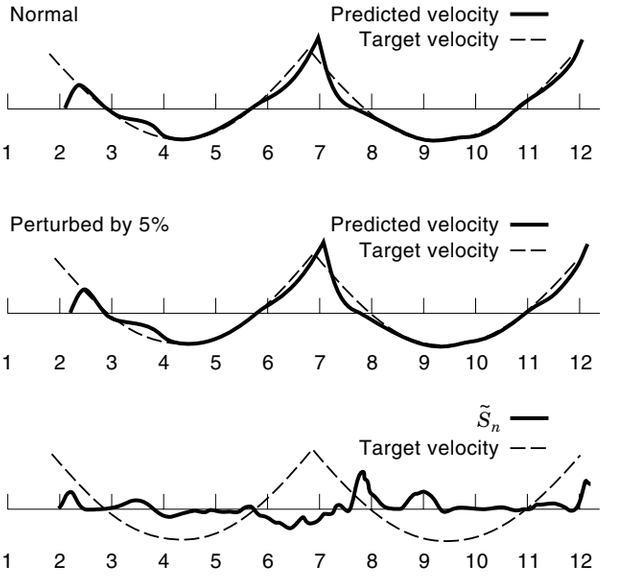

Figure 17. Semirelative sensitivity function of the predictor for changes in the number of weights for a cubic waveform. [From D. R. Harvey and A. T. Bahill, Development and sensitivity analysis of adaptive predictor for human eye movement model, *Transaction of the Society for Computer Simulation,* December 1985. © 1985 by Simulation Councils, Inc., San Diego, CA. Reprinted by permission. (Ref. 20).]

The Effect of Parameter Changes on the Mean-Square Error

Our semirelative sensitivity analysis gives a measure of how changing a parameter affects the model, and it shows when the parameter exerts its greatest influence. For our second sensitivity analysis, we considered the effect on the model's performance of changing each parameter over a range of values. Each parameter was given values above and below the nominal values; the velocity MSE between the model's output and the target was computed for each change. For the predictor, the filter's mean-square error (MSE) was computed between the velocity of the target 150 ms in the future and the velocity predicted by the adaptive predictor. The MSE were then plotted against the parameter values.

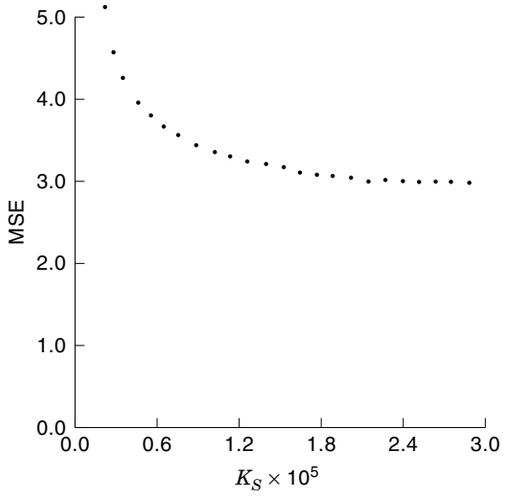

Figure 18. The MSE of the predictor as a function of changes in the proportionality constant. [From D. R. Harvey and A. T. Bahill, Development and sensitivity analysis of adaptive predictor for human eye movement model, *Transaction of the Society for Computer Simulation,* December 1985. © 1985 by Simulation Councils, Inc., San Diego, CA. Reprinted by permission. (Ref. 20).]

The Predictor's Sensitivity to Changes in Parameters

The effect of changes in the proportionality constant on the predictor was studied first. As the proportionality constant in Fig. 18 became larger, the filter's MSE became smaller. According to the misadjustment algorithm, the larger the value of k_s, the larger the misadjustment. This appears to disagree with this figure. However, the MSE for the figure was taken during the first 12 s of the simulation; therefore, the start-up transients are influencing the error. The larger the value of k_s, the faster the filter adapts; for smaller k_s the filter takes longer to converge, but does not converge to a solution with smaller error. Therefore, in the figure, the large MSE for a small k_s results because the filter takes longer to converge to the optimal solution. With the larger k_s values, the filter is converging rapidly and appears to have a smaller error. If k_s were increased even more, the error would also begin to increase. When we made the filter's task easier, by eliminating the start-up transient and only studying the steady-state behavior, we found that the filter's MSE increased with k_s as expected.

Our detailed analysis also showed a larger MSE for the cubic waveform compared to the sinusoidal waveform. This result is not unexpected since the cubic is a waveform that is of higher order than the sine wave and because the misadjustment is proportional to the expected value of the input signal.

Referring to Fig. 19, the MSE of the predictor is shown as function of the number of weights in the adaptive filter. According to the misadjustment algorithm, as the number of weights increases, so does the misadjustment of the filter. The curves here show the filter's error decreasing until 15 weights and then rising slightly before falling off after 40 weights. Because the adaptive filters use a tapped delay-line input signal, as the number of weights is increased, the input signals for the adaptive and slave filters begin to overlap. This improves the predictor's performance because the statistics of the two input signals are the same since the input signals are the same.

The increase in error between 15 and 40 weights shows the rise in error predicted by the misadjustment algorithm. However, after 40 weights the statistics of the input signals for the two filters begin to get close enough that the error drops off. The input signals for the two filters begin overlapping after 30 weights, which is approximately where the curves peak.

The effect of changing the prediction time and the signal's frequency were also studied. Figure 20 shows the predictor's

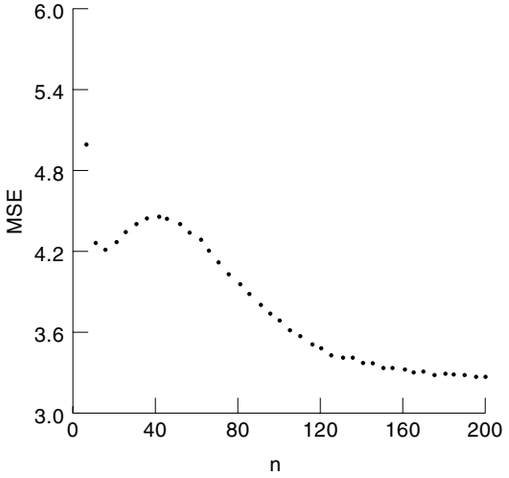

Figure 19. The MSE of the predictor as a function of changes in the number of weights for a cubic waveform. [From D. R. Harvey and A. T. Bahill, Development and sensitivity analysis of adaptive predictor for human eye movement model, *Transaction of the Society for Computer Simulation,* December 1985. © 1985 by Simulation Councils, Inc., San Diego, CA. Reprinted by permission. (Ref. 20).]

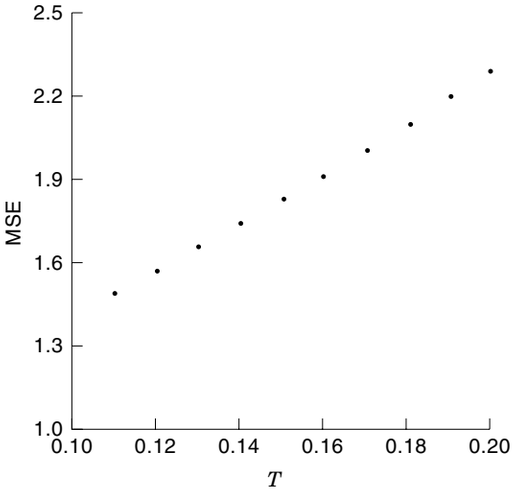

Figure 20. The change in the MSE of the predictor as the prediction time is changed. [From D. R. Harvey and A. T. Bahill, Development and sensitivity analysis of adaptive predictor for human eye movement model, *Transaction of the Society for Computer Simulation,* December 1985. © 1985 by Simulation Councils, Inc., San Diego, CA. Reprinted by permission. (Ref. 20).]

error as a function of prediction time. The error appears to be a linear function of the prediction time. The further into the future that is to be predicted, the worse the predictor does. We also computed that for changes in frequency, the faster the target moves the poorer the predictor does.

Summarizing, the predictor's performance is poorer as the proportionality constant is increased, although the error is a function of the time when the measurements were taken. For instance, in this study the start-up transients have not died down so the reverse statement appears true. For the weights, as the number of weights increased, the error also increased. The exception, seen in this work, occurs when a tapped delay-line input signal is used and the statistics of the input signals to the adaptive and slave filters are similar. The error of the predictor increases as the prediction time increases and as the input signal's frequency increases.

Discussion of Model and Least-Mean-Square Predictor

To create a model, we first determine the form and then derive parameter values. When possible we use physiological data to derive these values. A sensitivity analysis shows which parameters are the most and the least important so we can focus our efforts appropriately. In one of our final modeling stages we run a function minimization routine to adjust parameter values so that we get the least-squared error between the human and the model outputs.

Our model shown in Fig. 10 approximates the human smooth-pursuit system. Similarly, our simulation is only an approximation of the model in Fig. 10. For example, the model of Fig. 10 should be stable for any gain up to 2.3. But our simulation started to oscillate at 1.8. We found that we were getting 5° to 10° of artificial phase shift from the differentiators, the integrators, and even the summers. A smaller simulation step size would have obviously solved the problem; however, just being aware of the problem was also sufficient.

Our LMS predictor worked well except when discontinuities in the target waveform were present. For any desired accuracy, trade-offs could be made between the predicted gain and the number of weights. When this predictor was incorporated into our full eye movement model, the model was able to overcome its 150 ms delay and track targets with no latency, just like the human.

For optimal performance, 150 weights were used. Because the model gets a new target position every 5 ms, this means it uses the previous 750 ms of data for each calculation. We are not sure that the human uses this large a data window. Therefore, we also ran the model with only 15 weights. Even with this reduced number of weights, the model still performed as well as the human.

VALIDATE THE MODEL

The model tracks targets just as humans do. But in addition, we can do things with the model that we cannot do with humans. In Fig. 21 the top trace shows the model tracking with only the smooth-pursuit branch turned on, that is the saccadic branch and the adaptive predictor were turned off. The middle trace shows the model tracking with smooth pursuit and saccades only. Finally, the bottom trace shows the model tracking with smooth-pursuit saccades and the adaptive predictor. Only the bottom trace matches the tracking of normal humans.

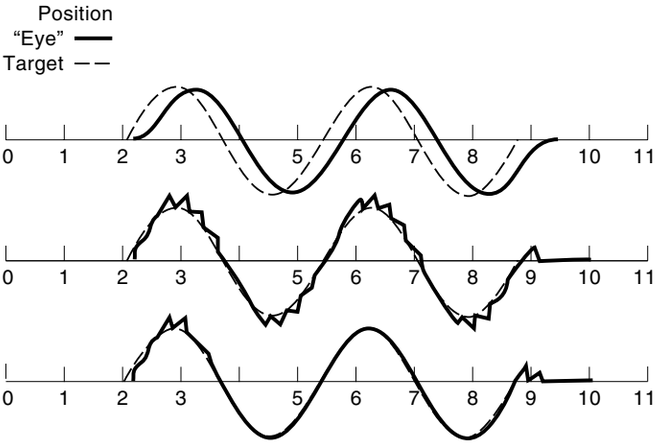

Figure 21. Position as a function of time for the TSAC model tracking a target with only the smooth-pursuit branch (top), smooth-pursuit and saccadic branches (middle), and all three branches turned on (bottom). Only the bottom trace resembles tracking of a normal human. Target movement was ±5°; time is in seconds. [From A. T. Bahill and J. D. McDonald, Model emulates human smooth pursuit system producing zero-latency target tracking, *Biol. Cybern.,* **48**: 218, 1983 (Ref. 19).]

Overcoming a Time Delay

To overcome a time delay and produce zero-latency tracking, you must (a) predict future target positions and (b) compensate for system dynamics, shown in Fig. 10. The latter means that you must have a model of the system that is updated when the system is changed by exercise, fatigue, or temperature variations.

INVESTIGATE ALTERNATIVE MODELS

We have just shown the development of the LMS adaptive predictor. It worked well, but we also compared it to alternative predictors. In our models we used the following predictors: (a) difference equations, for example, $r(n + 1) = Ar(n) + Br(n - 1)$, (b) menu selection, (c) LMS adaptive filters, (d) recursive least-square (RLS) filters, (e) Kalman filters, (f) adaptive lattice filters, and (g) a recursive least-square filter in conjunction with menu selection.

Difference equations were the simplest and least accurate. In the menu selection technique, the system has a menu of waveforms to choose from. In our simple models, we allowed sinusoidal, parabolic, cubic, and pseudorandom waveforms. The model then tracked the target and tried to identify the frequency, amplitude, and target waveform. It then used an equation for that waveform to help predict target motion. The seventh technique used a RLS filter to identify the waveform and then used equations off the menu to track the target. The other four techniques are typical filters described in digital signal processing literature.

When we first searched for literature on prediction we found very little. Then we realized that any digital filter could also be used for prediction. In fact, if you can either model a

system, identify a system, filter a signal, or predict a signal, then you can do the other three operations with no additional effort. All of our predictors allowed zero-latency tracking, just like the human. But, as will be discussed later, some matched other aspects of human behavior better than others.

The principle of Ockham's razor (48) states that if two models are equal in all respects except complexity, then the simpler model is the better one (see also http://pespmcl.vub.ac.be/OccamRaz.html). This is one reason why we like the menu selection predictors. They are simpler than the digital filters, which require complex matrix manipulation. Such calculations are fine for serial processing digital computers, but are not likely to be used by parallel processing analog computers such as the brain. This is one of the reasons that artificial neural networks are becoming so popular among physiological systems modelers (11).

USE THE MODEL FOR SOMETHING THAT IT WAS NOT DESIGNED FOR

A powerful technique for validating a model is to use it to simulate something that was unknown when the model was developed. Figure 22 shows some human tracking was that was noted to be unusual when the data were collected. The target position was a sinusoidal waveform, but the eye velocity waveform looks like that of a parabola. This behavior had not been seen before, and no explanation was apparent. But then we ran the menu selection model forcing it to choose the wrong waveform. Figure 23 shows the model tracking a sinusoidal waveform using a wrong guess of the parabolic waveform. These waveforms look very much like the human tracking of Fig. 22. This is another reason that we favor the menu selection predictors.

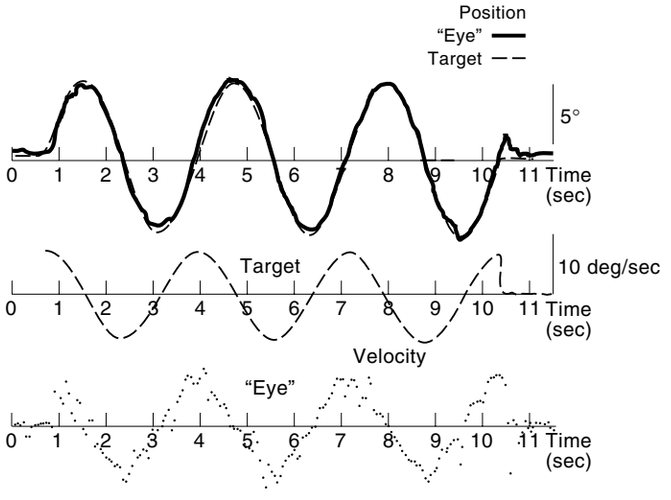

Figure 22. Human tracking of a sinusoidal target waveform. The top trace shows target position (dashed) and eye position (solid), the middle trace shows target velocity, and the bottom trace shows eye velocity. The eye velocity waveform does not match the target velocity waveform. [From A. T. Bahill and J. D. McDonald, Model emulates human smooth pursuit system producing zero-latency target tracking, *Biol. Cybern.,* **48**: 220, 1983 (Ref. 19).]

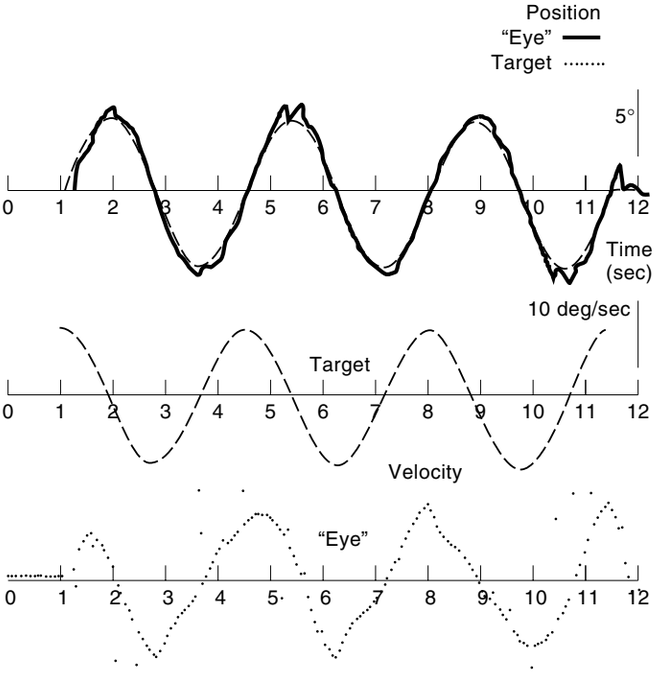

Figure 23. TSAC model with menu selection predictor tracking a sinusoidal target with an incorrect (parabolic) adaptive signal. The top trace shows target position (dashed) and model eye position (solid), the middle trace shows target velocity, and the bottom trace shows model eye velocity. [From A. T. Bahill and J. D. McDonald, Model emulates human smooth pursuit system producing zero-latency target tracking, *Biol. Cybern.,* **48**: 219, 1983 (Ref. 19).]

The Science of Baseball

To help validate the model, we used it to simulate something that was not used in the design of the model. Ted Williams, arguably the best hitter in the history of baseball, has described hitting a baseball as the most difficult single act in all of sports (49). The speed of the ball approaches 100 mph (45 m/s) (baseball is a game of inches, so the SI units come second in this section), producing angular velocities greater than 500°/s as the ball passes the batter. Humans cannot track targets moving faster than 70°/s (50) or perhaps 100°/s (51); yet, professional batters manage to hit the ball with force consistently and are able to "get a piece of the ball" on an average of more than 80% of their batting attempts. In this section we investigate how they do this by examining a professional baseball player tracking a "pitched ball," and we demonstrate the superiority of his eye movements and head–eye coordination to those of our other subjects.

Why did we want to study a batter tracking a baseball? We wanted to learn more about how the brain controls movement, and we therefore were searching for a situation in which a human was performing optimally. This condition is fulfilled by a professional baseball player tracking a pitched baseball.

In addition to the four basic eye movement systems, the batter can also use the head-movement system. Does he? Earlier studies by Bahill and LaRitz (41) have suggested several strategies for tracking a baseball: Track the ball with head movements and smooth-pursuit eye movements and fall be-

hind in the last 5 ft (1.5 m) of flight; track with eyes only, or with head only, and fall behind in the last 5 ft (1.5 m); track the ball over the first part of its trajectory with smooth-pursuit eye movements, make a saccadic eye movement to a predicted point ahead of the ball, continue to follow it with peripheral vision, and finally, at the end of the ball's flight, resume smooth-pursuit tracking with the ball's image on the fovea, the small area in the center of the retina that has fine acuity. We will examine each of these strategies.

The Simulated Fastball. To discover how well a batter tracked the ball, we had to be able to determine the position of the ball at all times, and thus we could not use a real pitcher or a throwing machine. Instead, we simulated the trajectory of a pitched baseball. We threaded a fishing line through a white plastic ball and stretched this line between two supports, which were set 80 ft (24 m) apart in order to accommodate the 60.5 ft (18 m) between pitcher and batter; a string was attached to the ball and wrapped around a pulley attached to a motor, so that when the motor was turned on, the string pulled the ball down the line at speeds between 60 mph (27 m/s) and 100 mph (45 m/s). The ball crossed the plate 2.5 ft (0.8 m) away from the subject's shoulders, simulating a high-and-outside fastball thrown by a left-handed pitcher to a right-handed batter. This, like all our constraints, was designed to give our subjects the best possible chance of keeping their eyes on the ball. A low curve ball thrown by a right-handed pitcher would have been much harder to track.

By controlling the speed of the motor and counting the rotations of the shaft, we could compute the position of the ball at every instant of time, and thus compare the position of the ball to the position of the batter's gaze. We define both positions in terms of the horizontal angle of the ball: the angle between the line of sight pointing at the ball and a line perpendicular to the subject's body (see Fig. 24). This angle is slightly more than 0° when the pitcher releases the ball, and it increases to 90° when the ball crosses the plate.

Tracking of a Professional Baseball Player. Figure 25 shows the tracking of a professional ballplayer Brian Harper, then a member of the Pittsburgh Pirates. He tracked the ball using head and eye movements, keeping his eye on the ball longer than our other subjects did. Our best-tracking student fell behind when the ball was 9 ft (2.7 m) in front of the plate. This professional baseball player was able to keep his position error below 2° until the ball was 5.5 ft (1.7 m) from the plate.

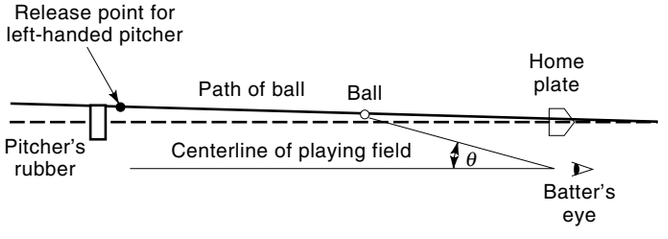

Figure 24. The horizontal angle of the ball, θ, as defined in this study, ranges from near 0 degrees when the pitcher releases the ball to 90 degrees when the ball crosses the plate. [From A. T. Bahill and T. LaRitz, Why can't batters keep their eyes on the ball, *Am. Sci.,* **72**: 250, 1984 (Ref. 41).]

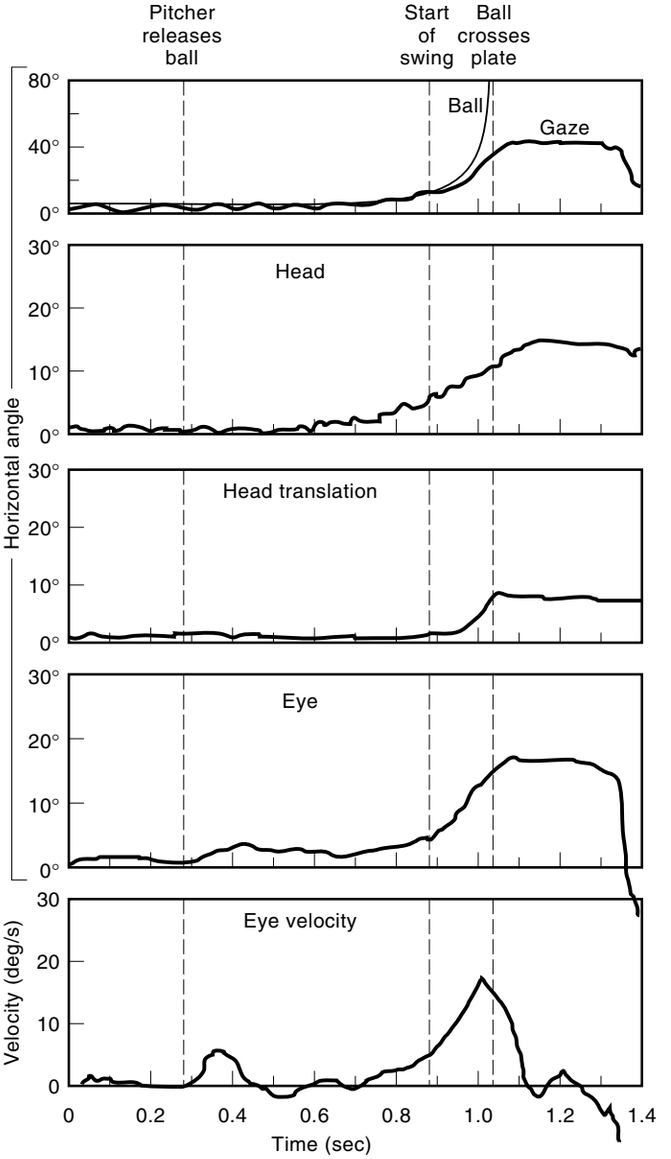

Figure 25. The success of a professional baseball player in tracking a simulated 60-mph (27 m/sec) pitch is shown in these graphs. The thin line in the top graph represents the horizontal angle of the ball, θ, as it would be seen by a right-handed batter facing a left-handed pitcher; the thick line represents the actual horizontal angle of gaze of the subject trying to track this ball. This gaze angle curve is generated by combining the horizontal head angle, the horizontal eye angle, and the head-translation angle, which represents the eye movement necessary to compensate for side-to-side and front-to-back movement of the head. Movements to the right appear as upward deflections. [From A. T. Bahill and T. LaRitz, Why can't batters keep their eyes on the ball, *Am. Sci.,* **72**: 251, 1984 (Ref. 41).]

The peak velocity of his smooth-pursuit tracking was 120°/s; at this point, his head velocity was 30°/s, thus producing a gaze velocity of 150°/s. In three simulated pitches to the professional baseball player, at speeds of 60 mph (27 m/s), 67 mph (30 m/s), and 70 mph (31 m/s) the overall tracking patterns were the same; his maximum smooth-pursuit eye velocities were 120, 130, 120°/s (52).

The gaze graph also takes into account the side-to-side and front-to-back movements of the head; such translations of the head can produce changes in the gaze angle (53). The data show that the contribution of the translation angle was slight until the ball was almost over the plate.

The professional baseball player had faster smooth-pursuit eye movements than our other subjects. In fact, he had faster smooth-pursuit eye movements than any reported in the literature. He also had better head–eye coordination, tracking the ball with equal-sized head and eye movements, whereas our other subjects usually had disproportionately large head or eye movements.

Keep Your Eye on the Ball. Although the professional baseball player was better than the college students at tracking the simulated fastball, it is clear from our simulations that batters, even professional batters, cannot *keep their eyes on the ball.* Our professional baseball player was able to track the ball until it was 5.5 ft (1.7 m) in front of the plate. This could hardly be improved on; we hypothesize that the best imaginable athlete could not track the ball closer than 5 ft (1.5 m) from the plate, at which point it would be moving three times faster than the fastest human could track. This finding runs contrary to one of the most often repeated axioms of batting instructors—"Keep your eye on the ball"—and makes it difficult to account for the widely reported claim that Ted Williams could sometimes see the ball hit his bat.

If Ted Williams were indeed able to do this, it could only be possible if he made an anticipatory saccade that put his eye ahead of the ball and then let the ball catch up to his eye. This was the strategy employed by the subject of Fig. 26; this batter observed the ball over the first half of its trajectory, predicted where it would be when it crossed the plate, and then made an anticipatory saccade that put his eye ahead of the ball. Using this strategy, the batter could see the ball hit the bat.

But why would a batter want to see the ball hit the bat? Because of his slow reaction time, he could not use the information gained in the last portion of the ball's flight to alter the course of the bat. We suggest that he uses the information to discover the ball's actual trajectory; that is, he uses it to learn how to predict the ball's location when it crosses the plate—how to be a better hitter in the future. The anticipatory saccade must be made before the end of the trajectory, because saccadic suppression prevents us from seeing during saccades (54,55). This suppression of vision extends about 20 msec after the saccade. So if you want to see the ball hit the bat, you must make your anticipatory saccade early in the trajectory.

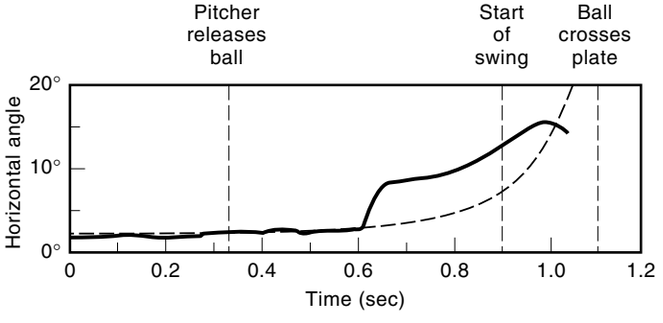

Figure 26. In order to see the ball hit his bat, this subject made an anticipatory saccade, indicated by the jump in the gaze angle (thick line) that put his eye ahead of the ball (thin line); as a result, the ball was on the fovea at the point of contact. The subject did not move his head until after the ball crossed the plate. [From A. T. Bahill and T. LaRitz, Why can't batters keep their eyes on the ball, *Am. Sci.,* **72**: 251, 1984 (Ref. 41).]

Head Movements and the Vestibulo-Ocular System. The vestibulo-ocular system is little used when tracking a baseball. However, in monitoring the eyes of our professional ball player, we did detect a small vestibulo-ocular movement to the left during the early part of the ball's trajectory, as the head was moving to the right; this appears as the slight dip between 0.5 s and 0.7 s in the eye position trace in Fig. 25. At this point, the head position was changing faster than the angular position of the ball, and the vestibulo-ocular eye movement compensated for the premature head movement. Why would the batter want to start his head movement early? The answer is that the head is heavier than the eye and consequently takes longer to get moving; therefore, in the beginning of the movement, as the head starts turning to the right ahead of the ball, the vestibular system in the inner ear signals the ocular system to make a compensating eye movement, thus giving his head a head start.

However, this vestibulo-ocular compensation must soon stop. In the end, the eye and head must both be moving to the right, and the batter must therefore suppress his vestibulo-ocular reflex so that the tracking head movement does not produce compensating eye movements that would take his eye off the ball. The professional baseball player was very good at suppressing his vestibulo-ocular reflex. Some of our student subjects did not make head movements until after the ball crossed the plate; others moved their heads very little. Perhaps they did this because they could not suppress the vestibulo-ocular reflex very well.

The fact that our professional baseball player used his head to help track the ball seems to violate another often repeated batting axiom, "Don't move your head." The professional made small tracking head movements in the range of 10° to 20°. He was able to suppress the vestibulo-ocular reflex for these movements, which were probably small enough to go unnoticed by a coach. However, body movements could produce head movements of 90° or more; it may be difficult to suppress the vestibulo-ocular reflex for these large body-induced movements, which along with correlated poor performance would be noticed by a coach. Therefore, we think the axiom should be protracted: "Don't let your body move your head, but it's okay to move your head a little in order to track the ball."

Batters do not use vergence eye movements. This is reasonable, since vergence eye movements are not needed to track the ball between 60 ft (18 m) and 6 ft (1.8 m) from the plate, and since there is not suficient time to make such movements between 6 ft (1.8 m) and the point of contact; indeed, our data contained no vergence eye movements. So any claim that a batter actually saw the ball hit the bat must be based on monocular vision; only the dominant eye tracks the ball.

Strategies. Sometimes our subjects used the strategy of tracking with head and eyes and falling behind in the last 5

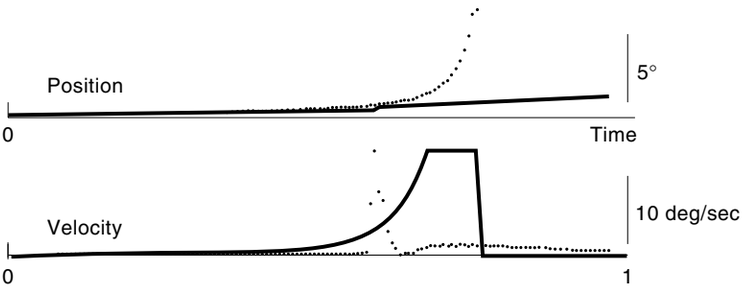

Figure 27. The model trying to track a baseball with the predictor turned off. The top trace is the angular position of the ball (dotted) and gaze (solid) and the bottom trace is velocity. The record is 1 s long. The model "kept its eye on the ball" until the ball was 9 ft (2.7 m) in front of the plate. This tracking resembles that of our best-tracking college students.

ft (1.5 m), and sometimes they used the strategy of tracking with head and eyes but also using an anticipatory saccade. It has been speculated that baseball players might use the latter strategy when they are learning the trajectory of a new pitch and use the former strategy when hitting home runs.

The professional baseball player tracked our simulated pitch better than any other subjects did. This superior tracking was due to (a) his use of both head and eye movements, (b) real fast smooth-pursuit eye movements, and (c) giving his head a head start.

Modeling Baseball Players. The eye movements of baseball players were not used in the development of the TSAC model. So if the model could simulate such eye movements, it would be a strong validation of the model. First, the limiter in the TSAC model was increased from its nominal value of 70°/s to the 130°/s that the professional baseball player exhibited. Figure 27 shows the model with the predictor turned off trying to track a baseball. It fell behind when the ball was nine feet from the plate. Figure 28 shows the model with the predictor turned on tracking a baseball. It was able to track the ball until the ball was 5.5 feet from the plate. The predictor makes a big difference. With the predictor, the model does as well as the professional baseball player whose data are shown in Fig. 25. The ball and gaze traces of Fig. 25 look very much like those of Fig. 28.

SUMMARY

The data presented in this section prompt the following summary about eye movements and baseball. You can't "keep your eye on the ball." Our best students could only track the ball until it was 9 feet in front of the plate. At that point, its annular velocity was so high that they fell behind. However, professional baseball players have superior eye movements.

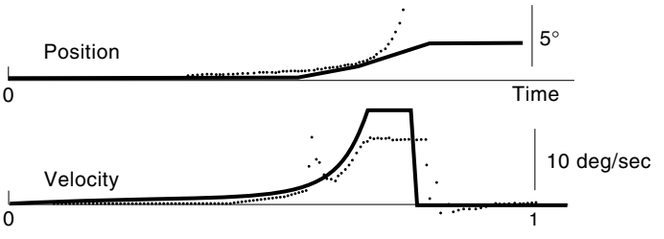

Figure 28. The model tracking a baseball with the predictor turned on. The model "kept its eye on the ball" until the ball was 5.5 ft (1.7 m) in front of the plate. This tracking resembles that of our professional baseball player.

They have better coordination of head and eye movements. They have faster smooth pursuit eye movements than any reported in the oculomotor literature. And they have better suppression of vestibulo-ocular eye movements. Because of these superiorities, the professional baseball player of this study was able to keep his eye on the ball until it was 5.5 feet in front of the plate. At this point, its annular velocity was so great that *no one* could track it farther. However, many people have reported that they have seen the ball hit their bat. This is possible using a different strategy: track the ball over the first half of its flight, then make a saccade that takes the eye off of the ball and aims the eye at the future site of the bat-ball collision. With this strategy, you can see the ball hit the bat.

The data presented in this section prompt the following summary about modeling human eye movements. Humans can overcome the time delays of the eye movement systems and track predictable visual targets with no latency or phase lag. To do the same, the TSAC model had to compensate for system dynamics and predict target velocity. Therefore, we think humans must use mental models of their eye movement systems to help compensate for system dynamics. These mental models must be adaptive, so that they can change due to muscular activity, fatigue, temperature, and so on. One good way to predict target velocity is menu selection. The baseball player's menu contains fastball, curveball, and slider.

ACKNOWLEDGMENT

I thank the anonymous reviewers of the manuscript for their sage comments.

BIBLIOGRAPHY

1. W. L. Chapman, A. T. Bahill, and A. W. Wymore, *Engineering Modeling and Design,* Boca Raton FL: CRC Press, 1992.
2. A. T. Bahill and W. J. Karnavas, The ideal baseball bat, *New Sci.,* **130** (1763): 26–31, 1991.
3. A. T. Bahill and M. Morna Freitas, Two methods for recommending bat weights, *Ann. Biomed. Eng.,* **23** (4): 436–444, 1995.
4. S. J. Yakowitz and F. Szidarovszky, *An Introduction to Numerical Computations,* New York: Macmillan, 1989.
5. A. T. Bahill, *Bioengineering: Biomedical, Medical and Clinical Engineering,* Englewood Cliffs, NJ: Prentice-Hall, 1981.
6. A. T. Bahill and B. Gissing, Re-evaluating systems engineering concepts using systems thinking, *IEEE Trans. Syst. Man Cybern.,* part C, **28**: November 1998.
7. C. Rashbass, The relationship between saccadic and smooth tracking eye movements, *J. Physiol.,* **159**: 326–338, 1961.

8. A. T. Bahill and J. D. McDonald, Smooth pursuit eye movements in response to predictable target motions, *Vision Res.,* **23**: 1573–1583, 1983.
9. G. Westheimer, Eye movement responses to a horizontally moving visual stimulus, *AMA Arch. Ophthalmol.,* **52**: 932–941, 1954.
10. L. Stark, G. Vossius, and L. R. Young, Predictive control of eye tracking movements, *IRE Trans. Hum. Factors Electron.,* **HFE-3**: 52–57, 1962.
11. R. E. Kettner et al., Prediction of complex two-dimensional trajectories by a cerebellar model of smooth pursuit eye movement, *J. Neurophysiol.,* **77**: 2115–2130, 1997.
12. P. J. Dallos and R. W. Jones, Learning behavior of the eye fixation control system, *IEEE Trans. Autom. Control,* **AC-8**: 218–227, 1963.
13. S. Yasui and L. Young, Perceived visual motion as effective stimulus to pursuit eye movement system, *Science,* **190**: 906–908, 1975.
14. L. Young, Pursuit eye movements—what is being pursued, in R. Baker and A. Berthoz (eds.), *Control of Gaze by Brain Stem Neurons,* pp. 29–36, Amsterdam: Elsevier/North-Holland, 1977.
15. M. Steinbach, Pursuing the perceived rather than the retinal stimulus, *Vision Res.,* **16**: 1371–1376, 1976.
16. A. Mack, R. Fendrich, and E. Wong, Is perceived motion a stimulus for smooth pursuit?, *Vision Res.,* **22**: 77–88, 1982.
17. R. Eckmiller, A Model of the Neural Network Controlling Foveal Pursuit Eye Movements, in A. F. Fuchs and W. Becker (eds.) *Progress in Oculomotor Research,* pp. 541–550, New York: Elsevier/North-Holland, 1981.
18. J. D. McDonald and A. T. Bahill, Zero-latency tracking of predictable targets by time-delay systms, *Int. J. Control,* **38**: 881–893, 1983.
19. A. T. Bahill and J. D. McDonald, Model emulates human smooth pursuit system producing zero-latency target tracking, *Biol. Cybern.,* **48**: 213–222, 1983.
20. D. R. Harvey and A. T. Bahill, Development and sensitivity analysis of adaptive predictor for human eye movement model, *Trans. Soc. Comput. Simul.,* **2**: 275–292, 1985.
21. D. E. McHugh and A. T. Bahill, Learning to track predictable target waveforms without a time delay, *Invest. Ophthalmol. Vis. Sci.,* **26**: 932–937, 1985.
22. H. Davson, *The Physiology of the Eye,* New York: Academic, 1976.
23. G. Marmount, Electrode clamp for squid axon: Studies on the axon membrane, *J. Cell. Comp. Physiol.,* **34**: 351–382, 1949.
24. K. S. Cole, Dynamic electrical characteristics of the squid axon membrane, *Arch. Sci. Physiol.,* **3**: 253–258, 1949.
25. L. Stark, *Neurological Control Systems, Studies in Bioengineering,* pp. 308–312, New York: Plenum, 1968.
26. R. B. Stein, What muscle variable(s) does the nervous system control in limb movements?, *Behav. Brain Sci.,* **5**: 535–577, 1982.
27. L. R. Young and L. Stark, Variable feedback experiments testing a sampled data model for eye tracking movements, *IEEE Trans. Hum. Factors Electron.,* **HFE-4**: 38–51, 1963.
28. H. J. Wyatt and J. Pola, Smooth pursuit eye movements under open-loop and closed-loop conditions, *Vision Res.,* **23**: 1121–1131, 1983.
29. H. J. Wyatt and J. Pola, The role of perceived motion in smooth pursuit eye movements, *Vision Res.,* **19**: 613–618, 1979.
30. A. T. Bahill and D. R. Harvey, Open-loop experiments for modeling the human eye movement system, *IEEE Trans. Syst. Man Cybern.,* **SMC-15**: 240–250, 1986.
31. H. Collewijn and E. P. Tamminga, Human fixation and pursuit in normal and open-loop conditions: Effects of central and peipheral retinal targets, *J. Physiol. (Lond.),* **379**: 109–129, 1986.
32. R. J. Leigh et al., Visual following during stimulation of an immobile eye (the open loop condition), *Vision Res.,* **22**: 1193–1197, 1982.
33. J. Pola and H. J. Wyatt, Offset dynamics of human smooth pursuit eye movements: Effects of target presence and subject attention, *Vision Res.,* **37**: 2579–2595, 1997.
34. P. Van Donkelarr, C. Fisher, and R. G. Lee, Adaptive modification of oculomotor pursuit influences manual tracking responses, *Neuroreport* **5**: 2233–2236, 1994.
35. M. F. W. Dubois and H. Collewijn, Optokinetic reactions in man elicited by localized retinal motion stimuli, *Vision Res.,* **19**: 1105–1115, 1979.
36. C. J. Gordon and J. E. Heath, Integration and control processing in temperature regulation, *Annu. Rev. Physiol.,* **48**: 595–612, 1986.
37. J. Ludbrook, Reflex control of blood pressure during exercise, *Annu. Rev. Physiol.,* **45**: 155–168, 1983.
38. D. J. C. Read and D. J. Henderson-Smart, Regulation of breathing in newborn during different behavioral states, *Annu. Rev. Physiol.,* **46**: 675–685, 1984.
39. D. A. Robinson, The mechanics of human smooth pursuit eye movements, *J. Physiol.,* **180**: 569–591, 1965.
40. J. S. Brodkey and L. Stark, New direct evidence against intermittency or sampling in human smooth pursuit eye movements, *Nature,* **218**: 273–275, 1968.
41. A. T. Bahill and T. LaRitz, Why can't batters keep their eyes on the ball, *Amer. Sci.,* **72**: 249–253, 1984.
42. L. Young, Pursuit eye tracking movements, in P. Bach-y-Rita, C. C. Collins, and J. Hyde (eds.), *The Control of Eye Movements,* New York: Academic, 1971, pp. 429–443.
43. B. Widrow, Adaptive filters, in R. E. Kalman, and N. DeClaris (eds.), *Aspects of Network and System Theory,* pp. 563–587, New York: Holt, Rinehart and Winston, 1971.
44. B. Widrow et al., Stationary and nonstationary learning characteristics of the LMS adaptive filter, *Proc. IEEE,* **64**: 1151–1162, 1976.
45. B. Widrow and S. D. Stearns, *Adaptive Signal Processing,* Englewood Cliffs, NJ: Prentice-Hall, 1985.
46. A. T. Bahill, J. R. Latimer, and B. T. Troost, Sensitivity analysis of linear homeomorphic model for human movement, *IEEE Trans. Syst. Man Cybern.,* **SMC-10**: 924–929, 1980.
47. W. J. Karnavas, P. Sanchez, and A. T. Bahill, Sensitivity analyses of continuous and discrete systems in the time and frequency domains, *IEEE Trans. Syst. Man Cybern.,* **SMC-23**: 488–501, 1993.
48. W. H. Jefferys and J. O. Berger, Ockham's razor and Bayesian analysis, *Am. Sci.,* **80**: 64–72, 1992.
49. T. Williams and J. Underwood, *The Science of Hitting,* New York; Simon and Schuster, 1982.
50. L. Schalen, Quantification of tracking eye movements in normal subjects, *Acta Otolaryngol.,* **90**: 404–413, 1980.
51. G. Zaccara et al., A new method for analyzing smooth-pursuit eye movements description of a microcomputer program and evaluation in healthy volunteers, *Ital. J. Neurol. Sci.,* **12**: 537–5445, 1991.
52. R. G. Watts and A. T. Bahill, *Keep Your Eye on the Ball: The Science and Folklore of Baseball,* New York: Freeman, 1990.
53. J. D. McDonald, A. T. Bahill, and M. B. Friedman, An adaptive control model for human head and eye movements while walking, *IEEE Trans. Syst. Man Cybern.,* **SMC-13**: 167–174, 1983.
54. L. Stark, J. A. Michael, and B. L. Zuber, Saccadic suppression: A product of the saccadic anticipatory signal, in C. R. Evans and T. B. Mulholland (eds), *Attention in Neurophysiology,* London, Butterworths, 1969, pp. 281–303.

55. E. Matin, Saccadic suppression and the dual mechanism theory of direction constancy, *Vision Res.,* **22**: 335–336, 1982.
56. A. T. Bahill and T. M. Hamm, Using open-loop experiments to study physiological systems with examples from the human eye movement systems, *News Physiol. Sci.,* **4**: 104–109, 1989.

A. TERRY BAHILL
University of Arizona